Development of the consistent second-order plate theory for transversely isotropic plates and its analytical assessment from the three-dimensional perspective

M. Kashtalyan*[1], R. Kienzler[2], M. Meyer-Coors[2]

[1]Centre for Micro- and Nanomechanics (CEMINACS), School of Engineering, University of Aberdeen, Fraser Noble Building, Aberdeen AB24 3UE, Scotland UK
[2]Bremen Institute of Mechanical Engineering (bi**me**), University of Bremen, Department of Production Engineering, Am Biologischen Garten 2, 28359 Bremen, Germany

Keywords: consistent plate theory; transversely isotropic plate; three-dimensional theory of elasticity; closed-form solution; Elliott's displacement potentials

Abstract
In this paper, the consistent second-order plate theory is developed for transversely isotropic plates. It is validated against the three-dimensional elasticity theory using a well-known benchmark problem of a simply-supported rectangular plate subjected to symmetric transverse sinusoidal loading. The choice of the benchmark problem is based on the fact that it allows for an exact three-dimensional elasticity solution to be derived in closed form. In this study, a closed-form solution based on Elliot's displacement potentials for transversely isotropic solids is specifically derived for validation purposes. Its equivalence to other closed-form analytical solutions is established. Expanding the closed-form analytical solution into a power-law series with respect to the non-dimensionalised plate thickness enables a direct term-by-term comparison with the consistent second-order plate theory solution and provides a valuable mechanism to validate the consistent plate theory for transversely isotropic plates in a purely analytical form. The term-by term comparison reveals that the first terms of the above power-law series coincide exactly with the expressions of the consistent second-order plate theory. In addition to the analytical validation, a numerical validation using the finite element method is performed. A comparative analysis of several plate theories for transversely isotropic plates demonstrates that the consistent plate theory can predict displacements and stresses in thick transversely isotropic plates with very high degree of accuracy, such that even for very thick plates with a thickness-to-length ratio of 0.5, the deviation from the three-dimensional elasticity solution is less than 1%.

*Corresponding author

1. Introduction

Many natural and manmade engineering materials possess direction-specific material properties and can be viewed as homogeneous anisotropic solids on the macroscopic scale. Design and analysis of structural components made of such materials require methods and tools that accurately take into account material's anisotropy as well as specifics of the component's geometry and function. Transverse isotropy is one of the commonly encountered types of anisotropy whereby a material has an axis of material symmetry perpendicular to the plane of isotropy and requires five independent elastic constants to describe its elastic response. Transversely isotropic plates and plate-like components can be found in many areas of engineering. A plate is a structural component whose thickness is much smaller than its in-plane dimensions. Design and analysis of plate-like components usually take place within the framework known as plate theory, which is a theoretical construction that takes advantage of the plate's small thickness and reduces a fully three-dimensional analysis to a two dimensional one. Two-dimensional plate theories, as long as they are employed within their range of applicability, can be used to study a great variety of static and dynamic behaviours, geometrical configurations, loading types and boundary conditions. The range of applicability for a specific plate theory is usually established through a comparison with full three-dimensional solutions for benchmark problems, for which such solutions are available. Although the development of plate theories began many decades ago, the research effort in this area still continues, as evidenced by recent publications (Wang et al. (2018), Wang et al. (2019), Tran et al. (2019), Liu et al. (2019), Furtmüller and Adam (2020), Joshan et al. (2020)), to name but a few.

Two-dimensional plate theories can be derived from a full three-dimensional elasticity theory using a number of approaches, as discussed in Kienzler and Kashtalyan (2020). Within the first, classical or engineering approach, a set of kinematical a priori assumptions is adopted for the displacement distribution in thickness direction, with additional assumptions concerning the stress distribution. Transverse shear strains are either neglected, or their influence is considered by means of shear-correction factors. A historical survey on classical plate theories may be found in, e.g., Szabo, (1987), whereas their mathematical justification is discussed, e.g., in Friesecke et al. (2002a, b). using the method of Γ-convergence developed by Giorgi (1975). Within the second, direct approach, all quantities "live" on a Cosserat-type surface endowed with a set of deformable directors attached to each point of the plane, whereas material parameters are identified through comparisons with a set of solutions of known test problems. A comprehensive review of Cosserat-type theories of plates and shells is given in Altenbach et al. (2010). The third approach develops lower-dimensional theories from the three-dimensional theory of elasticity by means of series expansion. In the works of Vekua (1955, 1985) series expansions with respect to a basis of Legendre polynomials were used. The so-called restricted-type theory for mixed plate-membrane problems, introduced by Steigmann (2008, 2012) and extended by Pruchnicki (2014), combines established modelling approaches of Koiter (1966, 1970a) with arguments taken from contributions based on Γ-convergence. Within the so called consistent approach (or uniform-approximation approach), which originates from works of Naghdi (1963), Koiter (1970b), Krätzig (1980) and Kienzler (1982) and will be used within this paper, plate theories are derived from the Euler-Lagrange equations of the truncated energy. Whatever the adopted approach, all plate theories are united by the fact that they attempt to describe a three-dimensional solid by a two-dimensional approximation, in which all quantities are defined on a surface.

The most rigorous way of constructing a two-dimensional approximation of a three-dimensional state of stress and a three-dimensional displacement field in a three-dimensional solid is provided by a group of plate theories known as consistent plate theories. In a consistent plate theory of a given order of approximation, all terms related to that order of approximation are retained in the three-dimensional representation of stresses and displacements. Such a logical and consistent approach produces the most accurate representation of stresses and displacements within the chosen order of approximation, enabling a better understanding of mechanical phenomena under investigation. The order of approximation depends on the nature of a phenomenon and the characteristic in-plane length measure associated with it. While for static problems, a second-order approximation may be sufficient, for dynamic phenomena, a higher-order approximation may be necessary because the in-plane measure such as the wavelength, for example, may be much smaller than the plate length (width).

A hierarchy of consistent plate theories has been developed in the works of Kienzler (2002), Kienzler (2004), Kienzler and Schneider (2012) and Schneider et al (2014). More recently, a method of constructing the displacement and stress field within a second-order consistent plate theory has been developed (Kienzler and Schneider, 2017). This, in turn, enabled a direct comparison of the consistent plate theory with the three-dimensional elasticity theory with a view to validate the former against the latter analytically. For a well-known benchmark problem of a simply supported rectangular plate subjected to symmetric sinusoidal loading, Kienzler and Kashtalyan (2020) derived an exact three-dimensional elasticity solution in closed form, expanded it into a Taylor series with respect to the non-dimensionalised plate thickness and carried out a direct term-by-term comparison with the consistent second-order plate theory solution. This term-by-term comparison revealed that the first terms of the above Taylor series coincide exactly with the expressions of the consistent plate theory. Due to this fact, the second-order plate theory can predict stresses and displacements in plates with a very high degree of accuracy, so that even for very thick plates with thickness-to-length ratio of 0.5, the deviation from a three-dimensional solution is less than 1%.

It should be pointed out that the above assessment of the consistent second-order plate theory was carried out for an isotropic plate. The aim of the present paper is to develop and validate analytically the consistent second-order plate theory for transversely isotropic plates. The objectives of the present paper are: (i) to present the development of the new consistent plate theory for transversely isotropic plates; (ii) to validate the new theory analytically using an exact three-dimensional elasticity solution, which is also developed in the paper specifically for this purpose; (iii) to demonstrate high accuracy of the new plate theory in comparison with the most widely used plate theories.

The new consistent second-order plate theory for transversely isotropic plates is validated against the three-dimensional elasticity theory using a well-known benchmark problem of a simply-supported rectangular plate subjected to symmetric transverse sinusoidal loading. The choice of the benchmark problem is based on the fact that it allows for an exact three-dimensional elasticity solution to be derived in closed form. In this study, a closed-form solution based on Elliot's displacement potentials is derived specifically for validation purposes. Its equivalence to other closed-form analytical solutions is established. Expanding the closed-form analytical solution into a power-law series with respect to the non-dimensionalised plate thickness enables a direct term-by-term comparison with the consistent second-order plate theory solution and provides a valuable mechanism to validate the consistent plate theory in purely analytical form. The term-by-term comparison reveals that the first terms of the above power-law series coincide exactly with the expressions of the consistent second-order plate theory. In addition to the analytical validation, a numerical validation using the finite element (FE) method is also performed. A comparative analysis of several plate theories for transversely isotropic plates demonstrates that the consistent plate theory can predict displacements and stresses in thick plates with a very high degree of accuracy, such that even for very thick plates with thickness-to-length ratio of 0.5, the deviation from the three-dimensional elasticity solution is less than 1%.

The paper is organised as follows. In Section 2, the problem statement is formulated and the necessary boundary conditions are specified. In Section 3, the boundary-value problem of Section 2 is solved within the framework of the consistent second-order plate theory for transversely isotropic plates. In Section 4, an exact closed-form three-dimensional elasticity solution using the displacement potentials method is derived for validation purposes. Its equivalence to other closed-form solutions available in the literature is addressed in the Appendix. In Section 5, the exact closed-form three-dimensional elasticity solution is expanded into a power series with respect to the normalised thickness parameter and a term-by-term comparison with the consistent plate theory solution of Section 3 is carried out. In Section 6, a comparative analysis of several plate theories for transversely isotropic plates is performed with the view to establish the range of applicability of the consistent second-order plate theory for transversely isotropic plates.

2. Problem statement

The problem statement is the same as in Kienzler and Kashtalyan (2020) since neither the load nor the boundary conditions depend on the material law. In order to keep the paper self-contained, we repeat the statement in an abridged manner.

We consider a rectangular plate $(a \times b)$ whose midplane is embedded in the (x_1, x_2)-plane of a Cartesian coordinate system. The plate continuum extends by $\pm h/2$ in x_3-direction. The plate is loaded along the plate faces $x_3 = \pm h/2$ by sinusoidal distributed transversal loads symmetrical with respect to the x_3-direction, (cf. Fig.1) i.e.,

$$q^+\left(x_\alpha, +\frac{h}{2a}\right) = q^-\left(x_\alpha, -\frac{h}{2a}\right) = \frac{1}{2} q_{mn} \sin\frac{m\pi x_1}{a} \sin\frac{n\pi x_2}{b}, \qquad (2.1)$$
$$q = q^+ + q^-.$$

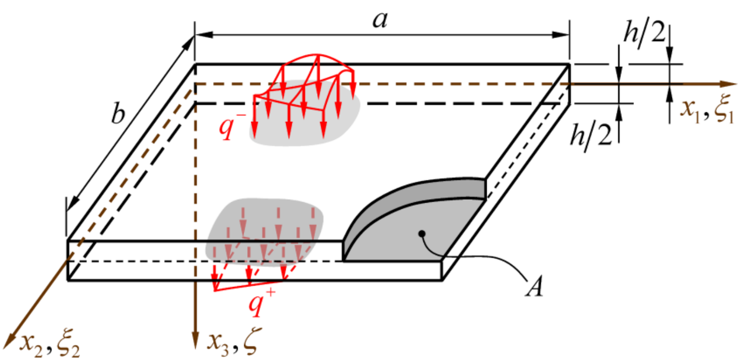

Fig. 1. Plate continuum

We introduce dimensionless coordinates and notations

$$\begin{aligned}
&\xi_1 = \frac{x_1}{a}, \\
&\xi_2 = \frac{x_2}{a}, \qquad \alpha\xi_2 = \frac{x_2}{b}, \\
&\zeta = \frac{x_3}{a}, \\
&\frac{\partial()}{\partial\xi_1} = ()_{,1}, \frac{\partial()}{\partial\xi_2} = ()_{,2}, \\
&\alpha = \frac{a}{b}, \\
&\gamma_{mn} = \sqrt{(m\pi)^2 + (n\pi\alpha)^2}.
\end{aligned} \qquad (2.2)$$

The summation convention is used over repeated indices. Latin indices $(i, j, k, \ldots)$ have the range $\{1, 2, 3\}$ and Greek indices (α, β, γ) range over $\{1, 2\}$. Displacements u_i, rotations ψ_α, stresses σ_{ij} and stress resultants $M_{\alpha\beta}, Q_\alpha$ are defined in the usual way as depicted in Figs. 2-4.

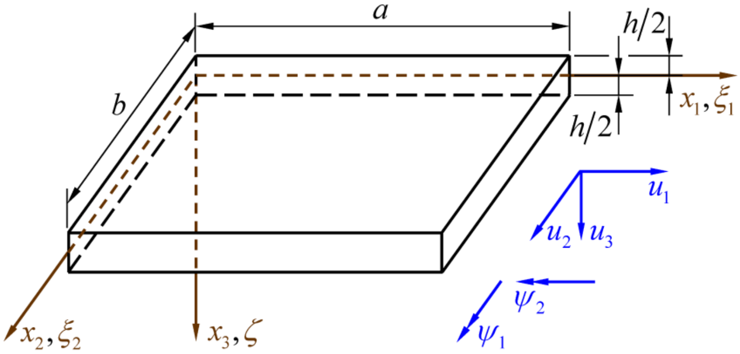

Fig. 2. Displacements and rotations

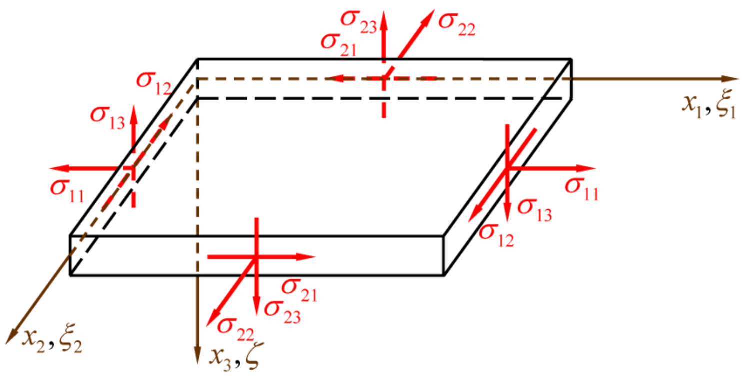

Fig. 3. Stresses at the plate continuum

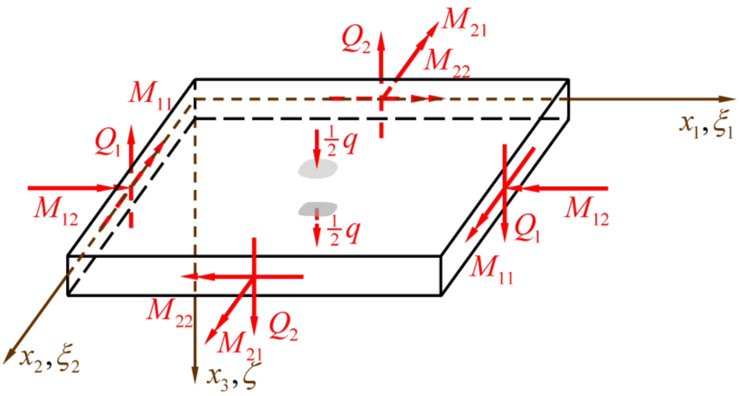

Fig. 4. Stress resultants and loads at the plate

The non-dimensionalised transverse displacement w is considered as energetic mean in Reissner's sense as

$$Q_\alpha w(\xi_1,\xi_2) = \int_{-\frac{h}{2a}}^{+\frac{h}{2a}} \sigma_{\alpha 3} u_3(\xi_1,\xi_2,\zeta) d\zeta \ . \ . \tag{2.3}$$

For details, cf., e.g., Kienzler and Schneider (2017).

The boundary conditions for constrained simply supported plates ("Klemmschneidenlagerung") are defined as

$$\begin{aligned}
\xi_1 &= 0,1: \quad M_{11} = 0, \quad \psi_2 = 0, \quad u_3 = 0; \\
\alpha\xi_2 &= 0,1: \quad M_{22} = 0, \quad \psi_1 = 0, \quad u_3 = 0; \\
\zeta &= \pm\frac{h}{2a}: \quad \sigma_{33} = \pm\frac{1}{2}q, \quad \sigma_{31} = \sigma_{32} = 0.
\end{aligned} \tag{2.4}$$

For the corresponding problem within the three-dimensional theory of elasticity, the following boundary conditions are to be satisfied

$$\begin{aligned}
\xi_1 &= 0,1: \quad \sigma_{11} = 0, \quad u_2 = 0, \quad u_3 = 0; \\
\alpha\xi_2 &= 0,1: \quad \sigma_{22} = 0, \quad u_1 = 0, \quad u_3 = 0; \\
\zeta &= \pm\frac{h}{2a}: \quad \sigma_{33} = \pm\frac{1}{2}q, \quad \sigma_{31} = \sigma_{32} = 0.
\end{aligned} \tag{2.5}$$

Within any second-order plate theory, a quantity ψ appears

$$\psi = \psi_{2,1} - \psi_{1,2}, \tag{2.6}$$

which is a measure for the transverse-shear deformation, cf. Reissner (1944), Reissner (1945), Schneider et al. (2014), Kienzler and Schneider (2017), Schneider and Kienzler (2017). Due to the prescribed boundary conditions (2.4), ψ vanishes identically

$$\psi(\xi_1,\xi_2) = 0 \tag{2.6}$$

and will not be considered here further, cf. Kienzler and Kashtalyan (2020).

3. Consistent plate theory solution for transversely isotropy

For monotropic plates, the second-order consistent plate theory has been fully established in Schneider and Kienzler (2017). The displacements have been developed in thickness direction with respect to a basis of generalized Legendre polynomials. The theory was specialized to transverse isotropy, the coefficients of the series expansion in Legendre polynomials were recalculated for a Taylor series expansion and the energetic average w was introduced[1]. The results of these extensive calculations are given in the following.

We adopt the Voigt notation as

$$\begin{bmatrix} \sigma_{11} \\ \sigma_{22} \\ \sigma_{33} \\ \sigma_{23} \\ \sigma_{31} \\ \sigma_{12} \end{bmatrix} = \begin{bmatrix} C_{11} & C_{12} & C_{13} & 0 & 0 & 0 \\ & C_{11} & C_{13} & 0 & 0 & 0 \\ & & C_{33} & 0 & 0 & 0 \\ symm. & & & C_{44} & 0 & 0 \\ & & & & C_{44} & 0 \\ & & & & & \frac{1}{2}(C_{11} - C_{12}) \end{bmatrix} \begin{bmatrix} \varepsilon_{11} \\ \varepsilon_{22} \\ \varepsilon_{33} \\ 2\varepsilon_{23} \\ 2\varepsilon_{31} \\ 2\varepsilon_{12} \end{bmatrix} \tag{3.1}$$

and introduce for further use the abbreviation

$$C_{11}^{*} = C_{11} - \frac{C_{13}^{2}}{C_{33}}, \tag{3.2}$$

which is named "reduced stiffness" in the textbooks on laminated composite structures, cf., e.g., Altenbach et al. (2004). We refer to the components of the stiffness "matrix" as C_{AB} $(A, B = 1, 2, ...6)$. In the special case of isotropy, we have

$$\begin{aligned} C_{11} &= C_{33} = \frac{E(1-\nu)}{(1+\nu)(1-2\nu)}, & C_{12} &= C_{13} = \frac{E\nu}{(1+\nu)(1-2\nu)}, \\ C_{44} &= C_{66} = \frac{E}{2(1+\nu)}, & C_{11}^{*} &= \frac{E}{1-\nu^{2}} \end{aligned} \tag{3.3}$$

with Young's modulus E and Poisson's ratio ν. We further define the dimensionless plate parameter as

$$c^{2} = \frac{h^{2}}{12a^{2}}, \tag{3.4}$$

which is usually a small quantity in plate theory since $h \ll a$.

With the two-dimensional Laplace operator $\Delta() = ()_{,\alpha\alpha}$, the governing plate differential equation is given as

[1] Kaya, S. (2018) Eine konsistente Plattentheorie zweiter Ordnung für den Fall der transversalen Isotropie. Bachelor Thesis. University of Bremen.

$$C_{11}^{*}c^2\Delta\Delta w = \frac{a}{h}\left(q - \frac{6}{5}c^2\left(\frac{C_{11}^{*}}{C_{44}} - \frac{C_{13}}{C_{33}}\right)\Delta q\right), \tag{3.5}$$

which reduces to

$$K\Delta\Delta w = a^3\left(q - \frac{6}{5}\frac{2-\nu}{1-\nu}c^2\Delta q\right) \tag{3.6}$$

for isotropic material, cf. Kienzler and Schneider (2017), Kienzler and Kashtalyan (2020).

The second, Reissner-type differential equation involving ψ and $\Delta\psi$ will not be considered here, since ψ vanishes identically for the given boundary-value problem as already mentioned. Also in the following, all contributions of ψ will be suppressed.

Similarly to Kienzler and Schneider (2017), the displacement fields can be evaluated a posteriori by satisfying the boundary conditions (2.4c) along the plate faces $\zeta = \pm h/(2a)$ and the homogeneous local equilibrium equations $\sigma_{ij,i} = 0$ with the following results

$$\begin{aligned}
\frac{u_\alpha}{a} = \zeta\Bigg\{ & -w,_\alpha + \frac{c^2}{C_{33}C_{44}}\left[\frac{3}{10}(C_{44}C_{13} - 5C_{11}^{*}C_{33}) - \frac{1}{6}\frac{\zeta^2}{c^2}(C_{44}C_{13} - C_{11}^{*}C_{33})\right]\cdot\Delta w,_\alpha \\
& + c^4\Bigg[-A_1 + \frac{1}{C_{33}^2C_{44}^2}\Bigg(+\frac{3}{40}C_{11}^{*}C_{33}(26C_{44}C_{13} - 25C_{11}^{*}C_{33}) \\
& + \frac{1}{20}\frac{\zeta^2}{c^2}\left(-C_{44}^2(5C_{11}^{*}C_{33} - C_{13}^2) - 11C_{44}C_{11}^{*}C_{33}C_{13} + 5C_{11}^{*2}C_{33}^2\right) \\
& + \frac{1}{120}\frac{\zeta^4}{c^4}\left(C_{44}^2(C_{11}^{*}C_{33} - C_{13}^2) + 3C_{44}C_{11}^{*}C_{33}C_{13} - C_{11}^{*2}C_{33}^2\right)\Bigg)\Bigg]\cdot\Delta\Delta w,_\alpha \\
& + O(c^6)\Bigg\},
\end{aligned} \tag{3.7}$$

$$\begin{aligned}
\frac{u_3}{a} = {} & w + c^2\frac{C_{13}}{C_{33}}\left(-\frac{3}{10} + \frac{1}{2}\frac{\zeta^2}{c^2}\right)\Delta w \\
& + c^4\Bigg[A_1 + \frac{1}{C_{33}^2C_{44}}\Bigg(\frac{3}{20}\frac{\zeta^2}{c^2}\left(C_{44}(5C_{11}^{*}C_{33} - C_{13}^2) + 5C_{11}^{*}C_{33}C_{13}\right) \\
& - \frac{1}{24}\frac{\zeta^4}{c^4}\left(C_{44}(C_{11}^{*}C_{33} - C_{13}^2) + C_{11}^{*}C_{33}C_{13}\right)\Bigg)\Bigg]\Delta\Delta w
\end{aligned}$$

$$
\begin{aligned}
&+c^6\Bigg[A_2+\frac{1}{2}\frac{\zeta^2}{c^2}\frac{C_{13}}{C_{33}}A_1 \qquad (3.8)\\
&\quad+\frac{1}{C_{33}^3C_{44}^2}\Bigg[\frac{3}{80}\frac{\zeta^2}{c^2}C_{11}^*C_{33}\left(-26C_{44}^2C_{13}+C_{44}(25C_{11}^*C_{33}-26C_{13}^2)+25C_{11}^*C_{33}C_{13}\right)\\
&\quad+\frac{1}{80}\frac{\zeta^4}{c^4}\left(C_{44}^2C_{13}(11C_{11}^*C_{33}-C_{13}^2)+C_{44}C_{11}^*C_{33}(-5C_{11}^*C_{33}+11C_{13}^2)-5C_{11}^{*2}C_{33}^2\,C_{13}\right)\\
&\quad+\frac{1}{720}\frac{\zeta^6}{c^6}\Big(C_{44}^2C_{13}(-3C_{11}^*C_{33}+C_{13}^2)+C_{44}C_{11}^*C_{33}(C_{11}^*C_{33}-3C_{13}^2)\\
&\qquad\qquad+C_{11}^{*2}\,C_{33}^2C_{13}\Big)\Bigg]\Bigg]\Delta\Delta\Delta w+O(c^8).
\end{aligned}
$$

Note that the displacements do not depend on C_{12}. As in the isotropic case, the constants A_1 and A_2 remain undetermined within the second-order theory. They do not contribute to the stress distribution. With (3.1), the stresses can be evaluated yielding

$$
\begin{aligned}
\sigma_{\alpha\beta}&=\frac{1}{C_{33}^2C_{44}}\zeta\Bigg\{-(C_{11}-C_{12})C_{33}^2C_{44}w_{,\alpha\beta}-C_{33}C_{44}(C_{12}C_{33}-C_{13}^2)\Delta w\delta_{\alpha\beta}\\
&\quad-\frac{1}{30}c^2\Big[9C_{33}(C_{11}-C_{12})(5C_{11}^*C_{33}-C_{13}C_{44})\Delta w_{,\alpha\beta}\\
&\quad+9\left(C_{44}C_{13}(C_{13}^2-C_{12}C_{33})-5C_{11}^*C_{33}(C_{13}(C_{13}+C_{44})-C_{12}C_{33})\right)\Delta\Delta w\delta_{\alpha\beta} \qquad (3.9)\\
&\quad-5\frac{\zeta^2}{c^2}\Big(C_{33}(C_{11}-C_{12})(C_{11}^*C_{33}-C_{13}C_{44})\Delta w_{,\alpha\beta}\\
&\quad+\left(C_{44}C_{13}(C_{13}^2-C_{12}C_{33})-C_{11}^*C_{33}(C_{13}(C_{13}+C_{44})-C_{12}\,C_{33})\right)\Delta\Delta w\delta_{\alpha\beta}\Big)\Big]\\
&\quad+O(c^4)\Bigg\},
\end{aligned}
$$

$$
\begin{aligned}
\sigma_{\alpha 3}&=\frac{1}{2}\frac{1}{C_{33}^2C_{44}}\left(3-\frac{\zeta^2}{c^2}\right)\Bigg\{-c^2C_{33}^2C_{44}C_{11}^*\Delta w_{,\alpha}\\
&\quad+\frac{1}{60}C_{11}^*C_{33}c^4\Big(3(-25C_{11}^*C_{33}+26C_{13}C_{44}) \qquad (3.10)\\
&\quad+5(C_{11}^*C_{33}-2C_{13}C_{44})\frac{\zeta^2}{c^2}\Big)\Delta\Delta w_{,\alpha}+O(c^6)\Bigg\}
\end{aligned}
$$

$$
\begin{aligned}
\sigma_{33}&=\frac{C_{11}^*C_{33}}{C_{33}^2C_{44}}\zeta\Bigg\{\frac{1}{6}c^2C_{33}C_{44}\left(9-\frac{\zeta^2}{c^2}\right)\Delta\Delta w\\
&\quad+\frac{1}{120}c^4\Bigg(9(25C_{11}^*C_{33}-26C_{13}C_{44})-6(5C_{11}^*C_{33}-6C_{13}C_{44})\frac{\zeta^2}{c^2} \qquad (3.11)
\end{aligned}
$$

$$+(C_{11}^* C_{33} - 2C_{13}C_{44})\frac{\zeta^4}{c^4}\Bigg) \Delta\Delta\Delta w^K + O(c^6)\Bigg\}$$

The stress distribution satisfies the boundary conditions along the plate faces

$$\begin{aligned}
&\sigma_{\alpha 3}\big|_{\pm\frac{h}{2a}} = 0 + O(c^6), \\
&\sigma_{33}\big|_{\pm\frac{h}{2a}} = \pm\frac{1}{2}q + O(c^6)
\end{aligned} \tag{3.12}$$

and the local homogeneous equilibrium equations

$$\begin{aligned}
&\sigma_{\beta\alpha,\beta} + \sigma_{3\alpha,3} = C_{11}^*\zeta\left(0 + O(c^4)\right) \\
&\sigma_{\alpha 3,\alpha} + \sigma_{33,3} = C_{11}^*\left(0 + O(c^6)\right).
\end{aligned} \tag{3.13}$$

The formulae (3.7)-(3.11) look quite complicated, but for given material constants, the pre-factors are just numbers and the equations have the same structure as in the isotropic case, cf. (3.10) and (3.11) in Kienzler and Kashtalyan (2020). For isotropy they coincide.

For the solution of (3.5) of our specific boundary-value problem (2.4) under the applied load (2.1), we employ the obvious ansatz

$$w = w_{mn} \sin m\pi\xi_1 \sin n\pi\alpha\xi_2 \tag{3.14}$$

and obtain from (3.5) with (2.2) for the constants w_{mn}

$$w_{mn} = \frac{12a^3 q_{mn}}{h^3\gamma_{mn}^4 C_{11}^*}\left(1 + \frac{6}{5}c^2\gamma_{mn}^2\left(\frac{C_{11}^*}{C_{44}} - \frac{C_{13}}{C_{33}}\right)\right). \tag{3.15}$$

The ansatz satisfies the differential equation (3.5) and the boundary conditions (2.4a and b) identically. Thus (3.14) with (3.15) is the exact analytical solution of our plate-boundary-value problem.

Next, we calculate the corresponding displacements form (3.7) and (3.8) and find

$$\frac{u_\alpha}{a} = \zeta\frac{12a^3 q_{mn}}{h^3\gamma_{mn}^4 C_{11}^*}\begin{Bmatrix} m\pi\cos m\pi\xi_1 \sin n\pi\alpha\xi_2 \\ n\pi\alpha \sin m\pi\xi_1 \cos n\pi\alpha\xi_2 \end{Bmatrix}$$
$$\Bigg\{-1 + \frac{1}{30}\frac{c^2\gamma_{mn}^2}{C_{33}C_{44}}\Bigg[9\left(3C_{44}C_{13} + C_{11}^*C_{33}\right) + 5\frac{\zeta^2}{c^2}\left(C_{44}C_{13} - C_{11}^*C_{33}\right)\Bigg]$$

$$-c^4\gamma_{mn}^4\left[A_1+\frac{1}{C_{33}^2C_{44}^2}\left[\frac{3}{200}\left(-24C_{44}^2C_{13}^2+C_{11}^*C_{33}\left(14C_{44}C_{13}+5C_{11}^*C_{33}\right)\right)\right.\right. \quad (3.16)$$

$$+\frac{1}{20}\frac{\zeta^2}{c^2}\left(C_{44}^2\left(5C_{11}^*C_{33}+3C_{13}^2\right)+3C_{44}C_{11}^*C_{33}C_{13}-C_{11}^{*2}C_{33}^2\right)$$

$$\left.\left.-\frac{1}{120}\frac{\zeta^4}{c^4}\left(C_{44}^2\left(C_{11}^*C_{33}-C_{13}^2\right)+3C_{44}C_{11}^*C_{33}C_{13}-C_{11}^{*2}C_{33}^2\right)\right]\right]+O(c^6)\Bigg\},$$

$$\frac{u_3}{a}=\frac{12a^3q_{mn}}{h^3\gamma_{mn}^4C_{11}^*}\sin m\pi\xi_1\sin n\pi\alpha\xi_2$$

$$\Bigg\{1-\frac{1}{10}\frac{c^2\gamma_{mn}^2}{C_{33}C_{44}}\left[3\left(3C_{44}C_{13}-4C_{11}^*C_{33}\right)+5\frac{\zeta^2}{c^2}C_{44}C_{13}\right]$$

$$+c^4\gamma_{mn}^4\left[A_1+\frac{1}{C_{33}^2C_{44}^2}\left[-\frac{9}{25}C_{44}C_{13}\left(C_{44}C_{13}-C_{11}^*C_{33}\right)\right.\right.$$

$$+\frac{3}{20}\frac{\zeta^2}{c^2}C_{44}\left(C_{44}(5C_{11}^*C_{33}+3C_{13}^2)+C_{11}^*C_{33}C_{13}\right)$$

$$\left.\left.-\frac{1}{24}\frac{\zeta^4}{c^4}C_{44}\left(C_{44}(C_{11}^*C_{33}-C_{13}^2)+C_{11}^*C_{33}C_{13}\right)\right]\right] \quad (3.17)$$

$$+c^6\gamma_{mn}^6\left[-A_2-\frac{1}{2}\frac{C_{13}}{C_{33}}\frac{\zeta^2}{c^2}A_1+\frac{6}{5}\frac{1}{C_{33}C_{44}}\left(C_{11}^*C_{33}-C_{44}C_{13}\right)A_1\right.$$

$$+\frac{1}{80}\frac{1}{C_{33}^3C_{44}^2}\left[\frac{1}{5}\frac{\zeta^2}{c^2}\left(6C_{44}^2C_{13}(5C_{11}^*C_{33}+12C_{13}^2)-3C_{44}C_{11}^*C_{33}(5C_{11}^*C_{33}+14C_{13}^2)-15C_{11}^{*2}C_{33}^2C_{13}\right)\right.$$

$$-\frac{\zeta^4}{c^4}\left(C_{44}^2C_{13}(7C_{11}^*C_{33}+3C_{13}^2)-C_{44}C_{11}^*C_{33}(C_{11}^*C_{33}-3C_{13}^2)-C_{11}^{*2}C_{33}^2C_{13}\right)$$

$$\left.\left.+\frac{1}{9}\frac{\zeta^6}{c^6}\left(C_{44}^2C_{13}(3C_{11}^*C_{33}-C_{13}^2)-C_{44}C_{11}^*C_{33}(C_{11}^*C_{33}-3C_{13}^2)-C_{11}^{*2}C_{33}^2C_{13}\right)\right]\right]+O(c^8)\Bigg\}$$

With (3.9 - 3.11) we find for the stresses

$$\sigma_{11}=\frac{a\zeta}{hc^2\gamma_{mn}^4}q_{mn}\sin m\pi\xi_1\sin n\pi\alpha\xi_2$$

$$\Bigg\{(m\pi)^2+\frac{C_{12}C_{33}-C_{13}^2}{C_{11}^*C_{33}}(n\pi\alpha)^2$$

$$+\frac{c^2\gamma_{mn}^2}{C_{33}C_{44}}\left[\frac{3}{10}(2C_{44}C_{13}-C_{11}^*C_{33})(m\pi)^2\right.$$

$$+\frac{3}{10}\frac{1}{C_{11}^*C_{33}}\left(C_{44}C_{13}(5C_{11}^*C_{33}+3C_{13}^2-3C_{12}C_{33})\right. \quad (3.18)$$

$$
\begin{aligned}
&-C_{11}^{*}C_{33}(C_{12}C_{33}-C_{13}^{2})\big)(n\pi\alpha)^{2} \\
&+\frac{1}{6}\frac{\zeta^{2}}{c^{2}}\Big(-(2C_{44}C_{13}-C_{11}^{*}C_{33})(m\pi)^{2} \\
&\qquad+\frac{1}{C_{11}^{*}C_{33}}\big(C_{44}C_{13}(-C_{11}^{*}C_{33}+C_{13}^{2}-C_{12}C_{33}) \\
&\qquad\qquad+C_{11}^{*}C_{33}(C_{12}C_{33}-C_{13}^{2})\big)(n\pi\alpha)^{2}\Big)\Big]+O(c^{4})\Big\},
\end{aligned}
$$

$$
\begin{aligned}
\sigma_{22}=&\frac{a\zeta}{hc^{2}\gamma_{mn}^{4}}q_{mn}\sin m\pi\xi_{1}\sin n\pi\alpha\xi_{2} \\
&\Big\{\frac{C_{12}C_{33}-C_{13}^{2}}{C_{11}^{*}C_{33}}(m\pi)^{2}+(n\pi\alpha)^{2} \\
&+\frac{c^{2}\gamma_{mn}^{2}}{C_{33}C_{44}}\Big[\frac{3}{10}\frac{1}{C_{11}^{*}C_{33}}\Big((C_{44}\,C_{13}(5C_{11}^{*}C_{33}+3C_{13}^{2}-3C_{12}C_{33}) \\
&\qquad-C_{11}^{*}C_{33}(C_{12}C_{33}-C_{13}^{2})\Big)(m\pi)^{2} \\
&\qquad+\frac{3}{10}(2C_{44}C_{13}-C_{11}^{*}C_{33})(n\pi\alpha)^{2}\big) \\
&\quad+\frac{1}{6}\frac{\zeta^{2}}{c^{2}}\Big(\frac{1}{C_{11}^{*}C_{33}}\big(C_{44}C_{13}(-C_{11}^{*}C_{33}+C_{13}^{2}-C_{12}C_{33}) \\
&\qquad\qquad+C_{11}^{*}C_{33}(C_{12}C_{33}-C_{13}^{2})\big)(m\pi)^{2} \\
&\qquad-(2C_{44}C_{13}-C_{11}^{*}C_{33})(n\pi\alpha)^{2}\Big)\Big]+O(c^{4})\Big\},
\end{aligned}
\tag{3.19}
$$

$$
\begin{aligned}
\sigma_{12}=&\frac{a\zeta}{hc^{2}\gamma_{mn}^{4}}q_{mn}m\pi\,n\pi\alpha\cos m\pi\xi_{1}\cos n\pi\alpha\xi_{2} \\
&\Big\{-\frac{C_{11}-C_{12}}{C_{11}^{*}}+\frac{c^{2}\gamma_{mn}^{2}}{C_{44}C_{11}^{*}C_{33}}(C_{11}-C_{12}) \\
&\Big[\frac{3}{10}(C_{11}^{*}C_{33}+3C_{13}C_{44})-\frac{1}{6}\frac{\zeta^{2}}{c^{2}}(C_{11}^{*}C_{33}-C_{13}C_{44})\Big]+O(c^{4})\Big\},
\end{aligned}
\tag{3.20}
$$

$$
\begin{aligned}
\sigma_{\alpha3}=&\frac{a}{2h\gamma_{mn}^{2}}q_{mn}\begin{Bmatrix}m\pi\cos m\pi\xi_{1}\sin n\pi\alpha\xi_{2}\\ n\pi\alpha\sin m\pi\xi_{1}\cos n\pi\alpha\xi_{2}\end{Bmatrix} \\
&\left(3-\frac{\zeta^{2}}{c^{2}}\right)\left[1-\frac{c^{2}\gamma_{mn}^{2}}{60C_{33}C_{44}}(C_{11}^{*}C_{33}-2C_{13}C_{44})\left(3-5\frac{\zeta^{2}}{c^{2}}\right)+O(c^{4})\right],
\end{aligned}
\tag{3.21}
$$

$$\sigma_{33} = \frac{a\zeta}{h} q_{mn} \sin m\pi\xi_1 \sin n\pi\alpha\xi_2$$

$$\left\{ \frac{1}{6}\left(9 - \frac{\zeta^2}{c^2}\right) - \frac{c^2\gamma_{mn}^2}{120} \frac{C_{11}^* C_{33} - 2C_{13}C_{44}}{C_{33}C_{44}} \left(9 - 6\frac{\zeta^2}{c^2} + \frac{\zeta^4}{c^4}\right) + O(c^4) \right\}. \quad (3.22)$$

4. Three-dimensional elasticity theory solution

Following Elliott (1948), displacements in a homogeneous transversely isotropic solid can be represented in terms of three quasi-harmonic functions ϕ_1, ϕ_2, ϕ_3 in the form

$$\begin{aligned} u_1 &= \frac{\partial\phi_1}{\partial x_1} + \frac{\partial\phi_2}{\partial x_1} + \frac{\partial\phi_3}{\partial x_2}, \\ u_2 &= \frac{\partial\phi_1}{\partial x_2} + \frac{\partial\phi_2}{\partial x_2} - \frac{\partial\phi_3}{\partial x_1}, \\ u_3 &= k_1 \frac{\partial\phi_1}{\partial x_3} + k_2 \frac{\partial\phi_2}{\partial x_3}, \end{aligned} \quad (4.1)$$

where

$$k_1 = \frac{C_{11}\theta_1 - C_{44}}{C_{13} + C_{44}}, \quad k_2 = \frac{C_{11}\theta_2 - C_{44}}{C_{13} + C_{44}} \quad (4.2)$$

and θ_1, θ_2 are the roots of the characteristic equation

$$C_{11}C_{44}\theta^2 + [C_{13}(2C_{44} + C_{13}) - C_{11}C_{33}]\theta + C_{33}C_{44} = 0. \quad (4.3)$$

The functions ϕ_1, ϕ_2, ϕ_3 satisfy the following quasi-harmonic equation

$$\begin{aligned} &\frac{\partial\phi_i^2}{\partial x_1^2} + \frac{\partial\phi_i^2}{\partial x_2^2} + \theta_i \frac{\partial\phi_i^2}{\partial x_3^2} = 0, \qquad \text{(no summation)} \\ &\theta_3 = \frac{2C_{44}}{C_{11} - C_{12}} \end{aligned} \quad (4.4)$$

The constant θ_3 represents the ratio between the shear moduli in the plane of isotropy and the plane normal to it. For isotropic materials it is equal to unity. For transversely isotropic materials it can be viewed as an anisotropy parameter that characterises the degree of anisotropy exhibited by the material. For example, mica gneiss with elastic properties $C_{11} = 89.73$ GPa, $C_{12} = 22.21$ GPa, $C_{13} = 23.50$ GPa, $C_{33} = 65.86$ GPa, $C_{44} = 24$ GPa (Hakala et al, 2007) has the anisotropy parameter $\theta_3 = 0.71$.

The expressions for stresses in the homogeneous transversely isotropic solid can be derived by substituting (4.1a-c) into the linearised strain-displacement relations and stress-strain relations (3.1)

$$
\begin{aligned}
\sigma_{11} &= \sum_{i=1}^{2}\left[C_{11}\frac{\partial^2\phi_i}{\partial x_1^2}+C_{12}\frac{\partial^2\phi_i}{\partial x_2^2}+C_{13}k_i\frac{\partial^2\phi_i}{\partial x_3^2}\right]+(C_{11}-C_{12})\frac{\partial^2\phi_3}{\partial x_1\partial x_2}\\
\sigma_{22} &= \sum_{i=1}^{2}\left[C_{12}\frac{\partial^2\phi_i}{\partial x_1^2}+C_{11}\frac{\partial^2\phi_i}{\partial x_2^2}+C_{13}k_i\frac{\partial^2\phi_i}{\partial x_3^2}\right]-(C_{11}-C_{12})\frac{\partial^2\phi_3}{\partial x_1\partial x_2}\\
\sigma_{33} &= \sum_{i=1}^{2}\left[C_{13}\frac{\partial^2\phi_i}{\partial x_1^2}+C_{13}\frac{\partial^2\phi_i}{\partial x_2^2}+C_{33}k_i\frac{\partial^2\phi_i}{\partial x_3^2}\right]\\
\sigma_{23} &= \sum_{i=1}^{2}\left[(k_i+1)C_{44}\frac{\partial^2\phi_i}{\partial x_2\partial x_3}\right]-C_{44}\frac{\partial^2\phi_3}{\partial x_1\partial x_3}\\
\sigma_{13} &= \sum_{i=1}^{2}\left[(k_i+1)C_{44}\frac{\partial^2\phi_i}{\partial x_1\partial x_3}\right]+C_{44}\frac{\partial^2\phi_3}{\partial x_2\partial x_3}\\
\sigma_{12} &= \sum_{i=1}^{2}\left[(C_{11}-C_{12})\frac{\partial^2\phi_i}{\partial x_1\partial x_2}\right]+\frac{1}{2}(C_{11}-C_{12})\left[\frac{\partial^2\phi_3}{\partial x_2^2}-\frac{\partial^2\phi_3}{\partial x_1^2}\right]
\end{aligned}
\qquad (4.5)
$$

The form of the quasi-harmonic functions depends on the specific boundary-value problem to be solved. For our problem under consideration, load distribution given by (2.1) and boundary conditions specified by (2.5), the three quasi-harmonic functions can be chosen in the form

$$
\begin{aligned}
\phi_1 &= \left(C_1\cosh\lambda_1 x_3 + C_2\sinh\lambda_1 x_3\right)\sin\frac{\pi m x_1}{a}\sin\frac{\pi n x_2}{b},\\
\phi_2 &= \left(C_3\cosh\lambda_2 x_3 + C_4\sinh\lambda_2 x_3\right)\sin\frac{\pi m x_1}{a}\sin\frac{\pi n x_2}{b},\\
\phi_3 &= \left(C_5\cosh\lambda_3 x_3 + C_6\sinh\lambda_3 x_3\right)\cos\frac{\pi m x_1}{a}\cos\frac{\pi n x_2}{b},\\
\lambda_i &= \sqrt{\frac{1}{\theta_i}\left[\left(\frac{\pi m}{a}\right)^2+\left(\frac{\pi n}{b}\right)^2\right]},\quad i=1,2,3.
\end{aligned}
\qquad (4.6)
$$

with θ_i given by (4.3) and (4.4b), provided the roots of the characteristic equation (4.3) are real. This choice of form for the harmonic functions ϕ_k $(k=1,2,3)$ allows for the boundary conditions (2.5a,b) at the edges of the plate to be satisfied identically. The six unknown constants C_k $(k=1,\dots,6)$ in (4.6) are found from the boundary conditions (2.5c) at the top and bottom surfaces of the plate. For the problem formulated in Section 2, they are found to be

$$C_1 = 0, \quad C_2 = \frac{q_{mn}}{2}\frac{\beta_2}{\beta_3}, \quad C_3 = 0, \quad C_4 = -\frac{q_{mn}}{2}\frac{\beta_1}{\beta_3}, \quad C_5 = 0, \quad C_6 = 0, \tag{4.7}$$

where

$$\begin{aligned}
\beta_1 &= (k_1+1)\lambda_1 \cosh(0.5\lambda_1 h), \\
\beta_2 &= (k_2+1)\lambda_2 \cosh(0.5\lambda_2 h), \\
\beta_3 &= \left[C_{33}k_1\lambda_1^2 - C_{13}\left(\left(\frac{\pi m}{a}\right)^2 + \left(\frac{\pi n}{b}\right)^2\right)\right] \\
&\quad (k_2+1)\lambda_2 \cosh(0.5\lambda_2 h)\sinh(0.5\lambda_1 h) \\
&\quad + \left[C_{13}\left(\left(\frac{\pi m}{a}\right)^2 + \left(\frac{\pi n}{b}\right)^2\right) - C_{33}k_2\lambda_2^2 \right] \\
&\quad (k_1+1)\lambda_1 \cosh(0.5\lambda_1 h)\sinh(0.5\lambda_2 h).
\end{aligned} \tag{4.8}$$

In view of (4.7) and (4.8), Elliot's quasi-harmonic functions (4.6) can be simplified as

$$\begin{aligned}
\phi_1 &= \frac{q_{mn}}{2}\frac{\beta_2}{\beta_3}\sinh \lambda_1 x_3 \sin\frac{\pi m x_1}{a}\sin\frac{\pi n x_2}{b}, \\
\phi_2 &= -\frac{q_{mn}}{2}\frac{\beta_1}{\beta_3}\sinh \lambda_2 x_3 \sin\frac{\pi m x_1}{a}\sin\frac{\pi n x_2}{b}, \\
\phi_3 &= 0.
\end{aligned} \tag{4.9}$$

Substitution of (4.9) into (4.1) yields the following closed-form expressions for the displacements

$$\begin{aligned}
u_1 &= \frac{q_{mn}}{2}\frac{1}{\beta_3}\left(\frac{\pi m}{a}\right)[\beta_2 \sinh \lambda_1 x_3 - \beta_1 \sinh \lambda_2 x_3]\cos\frac{\pi m x_1}{a}\sin\frac{\pi n x_2}{b}, \\
u_2 &= \frac{q_{mn}}{2}\frac{1}{\beta_3}\left(\frac{\pi n}{b}\right)[\beta_2 \sinh \lambda_1 x_3 - \beta_1 \sinh \lambda_2 x_3]\sin\frac{\pi m x_1}{a}\cos\frac{\pi n x_2}{b}, \\
u_3 &= \frac{q_{mn}}{2}\frac{1}{\beta_3}[k_1\lambda_1\beta_2 \cosh \lambda_1 x_3 - k_2\lambda_2\beta_1 \cosh \lambda_2 x_3]\sin\frac{\pi m x_1}{a}\sin\frac{\pi n x_2}{b}.
\end{aligned} \tag{4.10}$$

Likewise, substitution of (4.9) into (4.5) yields closed form expressions for the stresses

$$\sigma_{11}=\frac{q_{mn}}{2}\frac{1}{\beta_3}\sin\frac{\pi m x_1}{a}\sin\frac{\pi n x_2}{b}$$

$$\left\{\beta_2\left[-C_{11}\left(\frac{\pi m}{a}\right)^2-C_{12}\left(\frac{\pi n}{b}\right)^2+C_{13}k_1\lambda_1^2\right]\sinh\lambda_1 x_3\right. \tag{4.11a}$$

$$\left.-\beta_1\left[-C_{11}\left(\frac{\pi m}{a}\right)^2-C_{12}\left(\frac{\pi n}{b}\right)^2+C_{13}k_2\lambda_2^2\right]\sinh\lambda_2 x_3\right\},$$

$$\sigma_{22}=\frac{q_{mn}}{2}\frac{1}{\beta_3}\sin\frac{\pi m x_1}{a}\sin\frac{\pi n x_2}{b}$$

$$\left\{\beta_2\left[-C_{12}\left(\frac{\pi m}{a}\right)^2-C_{11}\left(\frac{\pi n}{b}\right)^2+C_{13}k_1\lambda_1^2\right]\sinh\lambda_1 x_3\right. \tag{4.11b}$$

$$\left.-\beta_1\left[-C_{12}\left(\frac{\pi m}{a}\right)^2-C_{11}\left(\frac{\pi n}{b}\right)^2+C_{13}k_2\lambda_2^2\right]\sinh\lambda_2 x_3\right\},$$

$$\sigma_{33}=\frac{q_{mn}}{2}\frac{1}{\beta_3}\sin\frac{\pi m x_1}{a}\sin\frac{\pi n x_2}{b}$$

$$\left\{\beta_2\left[-C_{13}\left(\frac{\pi m}{a}\right)^2-C_{13}\left(\frac{\pi n}{b}\right)^2+C_{33}k_1\lambda_1^2\right]\sinh\lambda_1 x_3\right. \tag{4.11c}$$

$$\left.-\beta_1\left[-C_{13}\left(\frac{\pi m}{a}\right)^2-C_{13}\left(\frac{\pi n}{b}\right)^2+C_{33}k_2\lambda_2^2\right]\sinh\lambda_2 x_3\right\},$$

$$\sigma_{13}=\frac{q_{mn}}{2}\frac{C_{44}}{\beta_3}\left(\frac{\pi m}{a}\right)\cos\frac{\pi m x_1}{a}\sin\frac{\pi n x_2}{b} \tag{4.11d}$$
$$\left\{\beta_2(k_1+1)\lambda_1\cosh\lambda_1 x_3-\beta_1(k_2+1)\lambda_2\cosh\lambda_2 x_3\right\},$$

$$\sigma_{23}=\frac{q_{mn}}{2}\frac{C_{44}}{\beta_3}\left(\frac{\pi n}{b}\right)\sin\frac{\pi m x_1}{a}\cos\frac{\pi n x_2}{b} \tag{4.11e}$$
$$\left\{\beta_2(k_1+1)\lambda_1\cosh\lambda_1 x_3-\beta_1(k_2+1)\lambda_2\cosh\lambda_2 x_3\right\},$$

$$\sigma_{12}=\frac{q_{mn}}{2}\left(\frac{C_{11}-C_{12}}{\beta_3}\right)\left(\frac{\pi m}{a}\right)\left(\frac{\pi n}{b}\right)\cos\frac{\pi m x_1}{a}\cos\frac{\pi n x_2}{b} \tag{4.11f}$$
$$\left\{\beta_2\sinh\lambda_1 x_3-\beta_1\sinh\lambda_2 x_3\right\}.$$

It should be pointed out that Elliot's displacement potentials cannot be applied directly to isotropic materials. For $C_{11}=C_{33}$, $C_{44}=\frac{1}{2}(C_{11}-C_{13})$, c.f. (3.3), the two distinct single roots of the characteristic equation (4.3), that depend on the material moduli, collapse to the double root $\theta_1=\theta_2=1$ (independent of the elastic moduli). By a limit analysis $\theta_2\to\theta_1\to 1$, it can be shown that the displacements (4.10) and the stresses (4.11) transform smoothly to the equations given in Kienzler and Kashtalyan (2020) for isotropic materials. Also, if an isotropic material with Young's modulus E, Poisson's ratio ν and shear modulus $C_{66}=$ $G=\dfrac{E}{2(1+\nu)}$, is treated as a transversely isotropic material with (cf. 3.3) $C_{11}=C_{33}=\dfrac{E(1-\nu)}{(1+\nu)(1-2\nu)}$, $C_{12}=C_{13}=\dfrac{E\nu}{(1+\nu)(1-2\nu)}$ but with the exception that $C_{44}=kG$, where k is a parameter, then the three-dimensional solution based on Elliott's displacements potentials will numerically converge to the three-dimensional elasticity solution for an isotropic plate when $k\to 1$. It may be mentioned further that the transition from transversely isotropic to isotropic material is possible without any special treatment after Taylor expansion of (4.10) and (4.11) in thickness direction, what is carried out in the next section.

5. Taylor series expansion and comparison

Since the higher-order plate theories are Taylor-series expansions of N^{th} order of the exact solution of the three-dimensional theory of elasticity, cf. Schneider et al. (2014), we develop the exact solution into a power series in c^2 and compare both term by term. It is sufficient to consider the displacements u_i. If the terms of the second-order plate theory coincide with those of the series expansion of the three-dimensional solution, the stresses will also coincide term by term due to Hooke's law (3.1).

To start with, we rearrange (4.10 a-c) by replacing β_i and k_α in terms of λ_α and the components of the stiffness tensor (3.1). Details will be given in the Appendix. With the abbreviations

$$A(\lambda_1,\lambda_2,h)=\lambda_2\cosh\left(\frac{1}{2}\lambda_2 h\right)\sinh\left(\frac{1}{2}\lambda_1 h\right)-\lambda_1\sinh\left(\frac{1}{2}\lambda_2 h\right)\cosh\left(\frac{1}{2}\lambda_1 h\right), \quad (5.1)$$

$$\kappa=\frac{1}{a}\gamma_{mn} \quad (5.2)$$

we obtain with the dimensionless coordinates (2.2)

$$\begin{aligned}u_\alpha=&\frac{1}{2}q_{mn}\frac{C_{13}+C_{44}}{C_{44}}\begin{Bmatrix}\dfrac{m\pi}{a}\cos(m\pi\xi_1)\sin(n\pi\alpha\xi_2)\\ \dfrac{n\pi\alpha}{a}\sin(m\pi\xi_1)\cos(n\pi\alpha\xi_2)\end{Bmatrix}\\ &\frac{1}{A(\lambda_1,\lambda_2,h)(\lambda_2^2C_{33}+\kappa^2C_{13})(\lambda_1^2C_{33}+\kappa^2C_{13})}\\ &\Big\{\lambda_2(\lambda_1^2C_{33}+\kappa^2C_{13})\cosh\left(\frac{1}{2}\lambda_2 h\right)\sinh(\lambda_1 a\zeta)\end{aligned} \quad (5.3)$$

$$-\lambda_1(\lambda_2^2 C_{33}+\kappa^2 C_{13})\cosh\left(\frac{1}{2}\lambda_1 h\right)\sinh(\lambda_2 a\zeta)\Bigg\},$$

$$u_3=\frac{1}{2}q_{mn}\frac{C_{13}+C_{44}}{C_{44}}\sin(m\pi\xi_1)\sin(n\pi\alpha\xi_2)$$
$$\frac{1}{A(\lambda_1,\lambda_2,h)(\lambda_2^2 C_{33}+\kappa^2 C_{13})(\lambda_1^2 C_{33}+\kappa^2 C_{13})} \tag{5.4}$$
$$\lambda_1\lambda_2\Bigg\{(\lambda_2^2 C_{33}+\kappa^2 C_{13})\cosh\left(\frac{1}{2}\lambda_2 h\right)\cosh(\lambda_1 a\zeta)$$
$$-(\lambda_1^2 C_{33}+\kappa^2 C_{13})\cosh\left(\frac{1}{2}\lambda_1 h\right)\cosh(\lambda_2 a\zeta)\Bigg\}.$$

The constants λ_α may be expressed as

$$\lambda_\alpha=\kappa\sqrt{\frac{2C_{11}C_{44}}{C_{11}^* C_{33}-2C_{13}C_{44}\mp\sqrt{(C_{11}^* C_{33}-2C_{13}C_{44})^2-4C_{11}C_{33}C_{44}^2}}}. \tag{5.5}$$

Then it follows

$$\frac{1}{(\lambda_2^2 C_{33}+\kappa^2 C_{13})(\lambda_1^2 C_{33}+\kappa^2 C_{13})}=\frac{a^4}{\gamma_{mn}^4}\frac{C_{44}}{C_{11}^*(C_{13}+C_{44})C_{33}}. \tag{5.6}$$

The series expansion itself was performed with Mathematica and leads finally to the following result

$$\frac{u_\alpha}{a}=\frac{12a^3 q_{mn}}{h^3\gamma_{mn}^4 C_{11}^*}\zeta\begin{Bmatrix} m\pi\cos m\pi\xi_1\sin n\pi\alpha\xi_2 \\ n\pi\alpha\sin m\pi\xi_1\cos n\pi\alpha\xi_2 \end{Bmatrix}$$
$$\Bigg\{-1+\frac{1}{30}\frac{c^2\gamma_{mn}^2}{C_{33}C_{44}}\left[9(3C_{13}C_{44}+C_{11}^* C_{33})+5\frac{\zeta^2}{c^2}(C_{44}C_{13}-C_{11}^* C_{33})\right]$$
$$+\frac{1}{4200}\frac{c^4\gamma_{mn}^4}{C_{33}^2 C_{44}^2}\Big[9\Big(C_{44}^2(195C_{11}^* C_{33}+157C_{13}^2)+73C_{44}C_{11}^* C_{33}C_{13}-27C_{11}^{*2}C_{33}^2\Big) \tag{5.7}$$
$$-210\frac{\zeta^2}{c^2}\Big(C_{44}^2(5C_{11}^* C_{33}+3C_{13}^2)+3C_{44}C_{11}^* C_{33}C_{13}-C_{11}^{*2}C_{33}^2\Big)$$
$$+35\frac{\zeta^4}{c^4}\Big(C_{44}^2(C_{11}^* C_{33}-C_{13}^2)+3C_{44}C_{11}^* C_{33}C_{13}-C_{11}^{*2}C_{33}^2\Big)\Big]\Bigg\}$$

$$\frac{u_3}{a}=\frac{12a^3 q_{mn}}{h^3\gamma_{mn}^4 C_{11}^*}\sin m\pi\xi_1\sin n\pi\alpha\xi_2\Bigg\{1-\frac{1}{10}\frac{c^2\gamma_{mn}^2}{C_{33}C_{44}}\left[3(3C_{44}C_{13}-4C_{11}^* C_{33})+5\frac{\zeta^2}{c^2}C_{13}C_{44}\right]$$
$$+\frac{1}{4200}\frac{c^4\gamma_{mn}^4}{C_{33}^2 C_{44}^2}\Big[-9\Big[C_{44}^2(195C_{11}^* C_{33}+157C_{13}^2)+3C_{44}C_{11}^* C_{33}C_{13}+8C_{11}^{*2}C_{33}^2\Big]$$

$$+630\frac{\zeta^2}{c^2}C_{44}\left[C_{44}(5C_{11}^{*}C_{33}+3C_{13}^{2})+C_{11}^{*}C_{33}C_{13}\right]$$
$$\left.-175\frac{\zeta^4}{c^4}C_{44}\left[C_{44}(C_{11}^{*}C_{33}-C_{13}^{2})+C_{11}^{*}C_{33}C_{13}\right]\right]$$
$$+\frac{1}{126000}\frac{c^6\gamma_{mn}^6}{C_{33}^3C_{44}^3}\Big[-9\Big[C_{44}^3C_{13}(1195C_{11}^{*}C_{33}+791C_{13}^{2})+C_{44}^2(115C_{11}^{*2}C_{33}^2+391C_{11}^{*}C_{33}C_{13}^2)$$
$$+27C_{44}C_{11}^{*2}C_{33}^2C_{13}-32C_{11}^{*3}C_{33}^3\Big] \tag{5.8}$$
$$+135\frac{\zeta^2}{c^2}C_{44}\Big[C_{44}^2C_{13}(265C_{11}^{*}C_{33}+157C_{13}^{2})-C_{44}(35C_{11}^{*2}C_{33}^2-73C_{11}^{*}C_{33}C_{13}^2)$$
$$-27C_{11}^{*2}C_{33}^2C_{13}\Big]$$
$$-1575\frac{\zeta^4}{c^4}C_{44}\left[C_{44}^2C_{13}(7C_{11}^{*}C_{33}+3C_{13}^{2})-C_{44}C_{11}^{*}C_{33}(C_{11}^{*}C_{33}-3C_{13}^{2})-C_{11}^{*2}C_{33}^2C_{13}\right]$$
$$\left.+175\frac{\zeta^6}{c^6}C_{44}\left[C_{44}^2C_{13}(3C_{11}^{*}C_{33}-C_{13}^{2})-C_{44}C_{11}^{*}C_{33}(C_{11}^{*}C_{33}-3C_{13}^{2})-C_{11}^{*2}C_{33}^2C_{13}\right]\right]$$
$$\left.+O(c^8)\right\}$$

The comparison of (3.16), (3.17) with (5.7), (5.8), respectively leads to the conclusion that all terms not containing the constants A_1 and A_2 perfectly coincide. The constants A_1 and A_2, which would follow from higher-order plate theories, can now be calculated. By comparing equal coefficients, we find

$$A_1=-\frac{3}{1400}\frac{1}{C_{33}^2C_{44}^2}\left[C_{44}^2(195C_{11}^{*}C_{33}-11C_{13}^{2})+171C_{44}C_{11}^{*}C_{33}C_{13}+8C_{11}^{*2}C_{33}^2\right], \tag{5.9}$$

$$\begin{aligned}A_2=+\frac{1}{14000}\frac{1}{C_{33}^3C_{44}^3}\Big[&5C_{44}^3C_{13}(1643C_{11}^{*}C_{33}+79C_{13}^{2})\\&-C_{44}^2C_{11}^{*}C_{33}(6905C_{11}^{*2}C_{33}-6943C_{13}^{2})\\&-C_{11}^{*2}C_{33}^2(5841C_{44}C_{13}+320C_{11}^{*}C_{33})\Big].\end{aligned} \tag{5.10}$$

For isotropic materials, again, the constants (5.9) and (5.10) coincide with (5.5) and (5.6), respectively, of Kienzler and Kashtalyan (2020).

6. Parametric study

In Kienzler and Kashtalyan (2020), an extended parametric study was performed for isotropic plates comparing the results of the exact 3-D elasticity solution with those for the second-order consistent plate theory. Displacements and stresses had been compared and it turned out that the relative error was less than 1% even for “brick-like plates” with $h/a=1/2$. An extended parametric study[2] for transversely isotropic plates was performed for sinusoidal loads, constants loads, various plate thicknesses varying between $h/a = 1/20$ and $h/a = 1/2$, as well as different length-to-width ratios $a/b = 1.0, \quad 1.3, \quad 1.5, \quad 1.8, \quad 2.0$. It turned out, again, that the relative error between the 3-D elasticity solution and the consistent plate theory is far less than 1%. So, little insight can be gained from providing numerous tables and figures. Instead, using Kirchhoff-type and Reissner-type plate elements available in Abaqus as well as three-dimensional finite element (FE) simulation, we will show results for the transverse displacement u_3 in the middle of a quadratic plate $(\alpha = 1)$ at the midplane and along the normal, in table and figure formats respectively. The wave numbers m and n are set to one and the results are non-dimensionalized by

$$\bar{u}_3(\bar{\zeta}) = \frac{\pi^4 C_{11}^* h^3}{3 q_{11} a^3} \frac{u_3\left(\frac{1}{2}, \frac{1}{2}, \bar{\zeta}\right)}{a} \tag{6.1}$$

with the new thickness variable $\bar{\zeta}$

$$\zeta = \frac{h}{a}\bar{\zeta}, \qquad -\frac{1}{2} \le \bar{\zeta} \le +\frac{1}{2}. \tag{6.2}$$

The material is mica gneiss, with the parameters from Hakala et al. (2007) as

$$\begin{aligned} &C_{11} = 89.73 \text{ GPa}, \quad C_{12} = 22.21 \text{ GPa}, \\ &C_{13} = 23.50 \text{ GPa}, \quad C_{33} = 65.86 \text{ GPa}, \\ &C_{44} = 24 \text{ GPa} \end{aligned} \tag{6.3}$$

and

$$C_{11}^* = 81.34 \text{ GPa}. \tag{6.4}$$

The anisotropy parameter (4.4b) has the value of

$$\theta_3 = 0.71\,. \tag{6.5}$$

Mica gneiss, chosen here for illustrative purposes, is a moderately anisotropic rock. Generally, rocks are not as strongly anisotropic as wood and fibre-reinforced composites, and consequently moderate anisotropy in rocks is sometimes neglected. However this may lead to significant errors when estimating the in situ state of stress in rock formations, which in turn may have unintended environmental consequences if the said rock formation is considered, for example, as a possible site for a radioactive waste depository (Hakala et al, 2007). Rock plates are often used to study various static and dynamics phenomena in rocks, therefore the

[2] Farahani, P.A. (2019). Vergleich von analytischen und numerischen Lösungen des Plattenproblems im isotropen und transversal isotropen Fall. Bachelor Thesis. University of Bremen.

numerical values provided by this benchmark problem example may also be used for validation purposes in computational modelling and simulation of transversely isotropic rocks.

The elasticity solution is indicated by $\overline{u}_3^E$ and is taken from (5.4). The Abaqus 3-D simulation using C3D20R elements is denoted by $\overline{u}_3^A$, the Kirchhoff plate simulation by $\overline{u}_3^K$, the Reissner-plate simulation by $\overline{u}_3^R$ and the consistent plate calculation by $\overline{u}_3^P$.

The latter follows from (5.8) as

$$
\begin{aligned}
\overline{u}_3^P\left(\overline{\zeta}\right) = 1 &- \frac{h^2\pi^2}{a^2}\frac{1}{C_{33}C_{44}}\left[\frac{1}{20}(3C_{44}C_{13} - 4C_{11}^{*}C_{33}) + \overline{\zeta}^2 C_{44}C_{13}\right] \\
&+ \frac{h^4\pi^4}{a^4}\frac{1}{C_{33}^2C_{44}^2}\left[-\frac{1}{16800}\left(C_{44}^2\left(195C_{11}^{*}C_{33} + 157C_{13}^2\right) + 3C_{44}C_{11}^{*}C_{33}C_{13}\right.\right. \\
&\left. + 8C_{11}^{*2}C_{33}^2\right) + \frac{1}{20}\overline{\zeta}^2 C_{44}\left(C_{44}\left(5C_{11}^{*}C_{33} + 3C_{13}^2\right) + C_{11}^{*}C_{33}C_{13}\right) \\
&\left. - \frac{1}{6}\overline{\zeta}^4 C_{44}\left(C_{44}\left(C_{11}^{*}C_{33} - C_{13}^2\right) + C_{11}^{*}C_{33}C_{13}\right)\right] \\
&+ \frac{h^6\pi^6}{a^6}\frac{1}{C_{33}^3C_{44}^3}\left[-\frac{1}{3024000}\left(C_{44}^3C_{13}\left(1195C_{11}^{*}C_{33} + 791C_{13}^2\right)\right.\right. \\
&\left. + C_{44}^2\left(115C_{11}^{*2}C_{33}^2 + 391C_{11}^{*}C_{33}C_{13}^2\right) + 27C_{44}C_{11}^{*2}C_{33}^2C_{13} - 32C_{11}^{*3}C_{33}^3\right) \\
&+ \frac{1}{16800}\overline{\zeta}^2 C_{44}\left(C_{44}^2C_{13}\left(265C_{11}^{*}C_{33} + 157C_{13}^2\right) - C_{44}\left(35C_{11}^{*2}C_{33}^2 - 73C_{11}^{*}C_{33}C_{13}^2\right)\right. \\
&\left. - 27C_{11}^{*2}C_{33}^2C_{13}\right) \\
&- \frac{1}{120}\overline{\zeta}^4 C_{44}\left(C_{44}^2C_{13}\left(7C_{11}^{*}C_{33} + 3C_{13}^2\right) - C_{44}C_{33}C_{11}^{*}\left(C_{11}^{*}C_{33} - 3C_{13}^2\right)\right. \\
&\left. - C_{13}C_{33}^2(C_{11}^{*})^2\right) \\
&+ \frac{1}{90}\overline{\zeta}^6 C_{44}\left(C_{44}^2C_{13}\left(3C_{11}^{*}C_{33} - C_{13}^2\right) - C_{44}C_{33}C_{11}^{*}\left(C_{11}^{*}C_{33} - 3C_{13}^2\right)\right. \\
&\left.\left. - C_{13}C_{33}^2(C_{11}^{*})^2\right)\right] + O(c^8)
\end{aligned}
\tag{6.6}
$$

The results for $\overline{\zeta} = 0$ are shown in Table. 1, where $\Delta\%$ is defined as follows:

$$\Delta\% = \frac{\overline{u}_3^E - \overline{u}_3^X}{\overline{u}_3^E}\cdot 100\%, \quad X = A, K, R, P.$$

Table 1 Transverse displacements $\bar{u}_3$ for different plate theories

$\frac{h}{a}$	$\frac{1}{20}$	$\Delta\%$	$\frac{1}{10}$	$\Delta\%$	$\frac{1}{5}$	$\Delta\%$	$\frac{1}{3}$	$\Delta\%$	$\frac{1}{2}$	$\Delta\%$
$\bar{u}_3^E(0)$	1.015	-	1.061	-	1.243	-	1.659	-	2.412	-
$\bar{u}_3^A(0)$	1.015	0.07	1.061	0.06	1.242	0.06	1.659	0.04	2.411	0.06
$\bar{u}_3^K(0)$	0.999	1.52	0.999	5.79	0.999	19.56	1.002	39.73	0.999	58.54
$\bar{u}_3^R(0)$	1.016	-0.06	1.066	-0.43	1.267	-1.92	1.744	-5.11	2.671	-10.73
$\bar{u}_3^P(0)$	1.015	0.00	1.061	0.00	1.243	0.00	1.659	0.01	2.411	0.05

As evidenced by values presented in Table 1, the FE simulation is very accurate. Following a convergence study, a mesh size from 0.025 was deemed to be sufficiently accurate, i.e., 40 x 40 elements in ξ_1 and ξ_2 direction for a quadratic plate. In thickness direction, the number of elements was chosen depending on the plate thickness. For $h/a = 1/20,\ 1/10,\ 1/5,\ 1/3$ and $1/2$, the number of elements in the thickness direction was taken as 2, 4, 8, 14 and 20, respectively.

As in the case of isotropy, the Kirchhoff-plate theory is applicable only for very thin plates. For $h/a = 1/10$, the error already exceeds 5% and for thicker plates the theory is not applicable anymore. Reissner's plate theory delivers still acceptable results for thick plates in the range of $h/a = 1/3$. The consistent second-order plate theory for a brick-like plate with $h/a = 1/2$ delivers very accurate results within an error of far less than 1%.

We note that the displacement values calculated using Abaqus, Kirchhoff plate theory and the consistent plate theories are smaller than the value obtained using 3-D elasticity theory, whereas for Reissner plate theory the opposite is true. A possible explanation for this trend is that a Reissner plate is more compliant producing a greater displacement in comparison to the elasticity solutions, because the stiffening effect due to transverse normal stresses is not completely taken into account. A Kirchhoff plate is stiffer, i.e. the displacements are smaller in comparison to the elasticity solution since the deformation due to transverse shear are neglected (shear-rigid plate theory).

Finally, we will show the development of $\bar{u}_3^P(\bar{\zeta})$ for different ratios of h/a for different approximation orders. To this extent, we cut equation (6.6) after the constant term: $\bar{u}_3^0$, after the $(h/a)^2$ term: $\bar{u}_3^1$, after the $(h/a)^4$ term: $\bar{u}_3^2$ and after the $(h/a)^6$ term: $\bar{u}_3^3$

$$\bar{u}_3^0(\bar{\zeta}) = 1 \tag{6.7}$$

$$\bar{u}_3^1(\bar{\zeta}) = 1 - \frac{h^2\pi^2}{a^2}\frac{1}{C_{33}C_{44}}\left[\frac{1}{20}(3C_{44}C_{13} - 4C_{11}^*C_{33}) + \bar{\zeta}^2 C_{44}C_{13}\right] \tag{6.8}$$

$$\bar{u}_3^2(\bar{\zeta}) = 1 - \frac{h^2\pi^2}{a^2}\frac{1}{C_{33}C_{44}}\left[\frac{1}{20}(3C_{44}C_{13} - 4C_{11}^*C_{33}) + \bar{\zeta}^2 C_{44}C_{13}\right]$$
$$+\frac{h^4\pi^4}{a^4}\frac{1}{C_{33}^2C_{44}^2}\left[-\frac{1}{16800}\left(C_{44}^2(195C_{11}^*C_{33} + 157C_{13}^2) + 3C_{44}C_{11}^*C_{33}C_{13}\right.\right.$$
$$\left.+8C_{11}^{*2}C_{33}^2\right) + \frac{1}{20}\bar{\zeta}^2 C_{44}\left(C_{44}(5C_{11}^*C_{33} + 3C_{13}^2) + C_{11}^*C_{33}C_{13}\right)$$
$$\left.-\frac{1}{6}\bar{\zeta}^4 C_{44}\left(C_{44}(C_{11}^*C_{33} - C_{13}^2) + C_{11}^*C_{33}C_{13}\right)\right]. \tag{6.9}$$

$$\bar{u}^3(\bar{\zeta}) = \bar{u}_3^P(\bar{\zeta}) \tag{6.10}$$

We plot the results in Fig. 5 versus $\bar{\zeta}$ for $h/a = 1/3$.

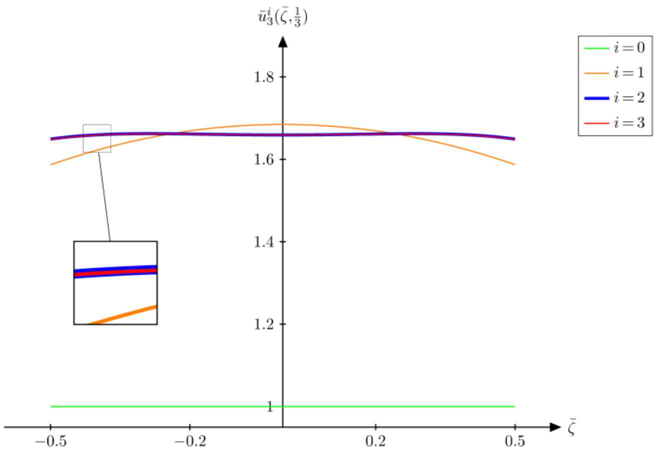

Fig. 5 Transverse displacement $\bar{u}_3^i$ for different approximation orders

The transverse displacement $\bar{u}_3^0$ represents the result of the classical solution and is equal to 1 (const.). The first-order approximation (quadratic parabola) improves the solution considerably, whereas the second-order approximation adjusts the displacement in a still visible manner. The third-order term, which is not fully fixed within the consistent second-order plate theory, results in a marginal improvement not visible in Fig. 5.

7. Conclusion

Following on from the Kienzler and Kashtalyan (2020) paper, in which the consistent second-order plate theory for isotropic plates was assessed from the perspective of the three-dimensional elasticity theory, in this paper, the consistent second-order plate theory has been developed for transversely isotropic plates. To validate the new theory analytically, closed form solutions for the benchmark problem of a simply supported rectangular plate under sinusoidal load were derived, both within the new consistent second-order plate theory as well as within the three-dimensional elasticity theory. For the latter, an approach based on displacement potential functions was used. The elasticity solution was expanded into a Taylor series, which enabled their term by term comparison in analytical form with the second-order plate solution. The Taylor series expansion with respect to the non-dimensionalised thickness-to-length ratio revealed that the formulae of the new plate theory coincide exactly with the first terms of the Taylor-series expansion of the three-dimensional elasticity solution.

Additionally, numerical comparisons were made with Kirchhoff's and Reissner's plate theories as well as FE simulations, for the special case of a quadratic plate under a single-wave sinusoidal loading. Numerical results demonstrated that the consistent second-order plate theory for transversely isotropic plates works remarkably well, so that even for thick plates with a thickness-to-length ratio equal to 0.5 – which are rather three-dimensional bricks than plates – the deviation from the three-dimensional elasticity solution is far less than 1%.

8. Acknowledgements

Financial support of this research by The Royal Society (UK) International Exchanges award (IE161021) and by the German Science Foundation (DFG) under Project-No. Ki 284/25-1 is gratefully acknowledged

9. References

Altenbach, J., Altenbach, H., Eremeyev, V. (2010) On generalized Cosserat-type theories of plates and shells: A short review and bibliography. Arch. Appl. Mech. 80: 73-92.

Altenbach, H., Altenbach, J., Kissing, W. (2004) Mechanics of composite structural elements. Berlin: Springer.

Elliott, H.A. (1948) Three-dimensional stress distributions in hexagonal aeolotropic crystals. Proceedings of the Cambridge Philosophical Society, 44: 522-553.

Friesecke, G., James, R. D., Müller, S. (2002a) A theorem on geometric rigidity and the derivation of nonlinear plate theory from three-dimensional elasticity. Commun. Pure Appl. Mat. 55: 1461-1506.

Friesecke, G., Müller, S., James, R. D. (2002b) Rigorous derivation of nonlinear plate theory and geometric rigidity. Comtes Rendus Math. 334: 173-178.

Furtmüller, T., Adam, C. (2020) An accurate higher order plate theory for vibrations of cross-laminated timber panels. Composite Structures, 239: 112017.

Giorgi, E. D. (1975) Sulla convergenza di alcune successioni di integrali del tipo dell'aera. Rend. Mat. Appl. 8: 277-294.

Joshan, Y.S., Santapuri, S., Grover, N. (2020) Analysis of laminated piezoelectric composite plates using an inverse hyperbolic coupled plate theory. Applied Mathematical Modelling, 82: 359-378.

Hakala, M., Kuula, H., Hudson, J.A. (2007) Estimating the transversely isotropic elastic intact rock properties for in situ stress measurement data reduction: A case study of the Olkiluoto mica gneiss, Finland. Int. J. of Rock Mechanics and Mining Sciences, 44: 14-46.

Hu, H.C. (1953) On the three-dimensional problems of the theory of elasticity of a transversely isotropic body. Scientia Sinica, 2: 145-151.
Kienzler, R. (1982) Eine Erweiterung der klassischen Schalentheorie; Der Einfluss von Dickenverzerrungen und Querschnittsverwölbungen. Ing. Arch. 52: 311-322. Extended version in: PhD Thesis, Technische Hochschule Darmstadt, Darmstadt (1980).
Kienzler, R. (2002) On consistent plate theories. Arch. Appl. Mech. 72: 229-247.
Kienzler, R. (2004) On consistent second-order plate theories. In: Kienzler, R., Altenbach, H., Ott, I. (Eds.) Theories of plates and shells: critical review and new applications. Springer, Berlin: 85-96.
Kienzler, R., Kashtalyan, M. (2020) Assessment of the consistent second-order plate theory for isotropic plates from the perspective of the three-dimensional theory of elasticity. Int. J. Solids Structures 185-186: 257-271.
Kienzler, R., Schneider, P. (2012) Consistent theories of isotropic and anisotropic plates. J. Theoret. Appl. Mech. 50: 755-768.
Kienzler, R., Schneider, P. (2017) Second-order linear plate theories: Partial differential equations, stress resultants and displacements. Int. J. Solids and Struct. 115-116: 14-26.
Kirchhoff, G. (1859) Über das Gleichgewicht und die Bewegung eines unendlich dünnen elastischen Stabes. Crelles J. angew. Math. 56: 283-313.
Koiter, W. (1966) On the nonlinear theory of thin elastic shells. Koninklijke Nederlandse Akademie van Wetenschapen, Proceedings, Series B 69: 1-54.
Koiter, W. (1970a) On the foundation of the linear theory of thin elastic shells. Koninklijke Nederlandse Akademie van Wetenschappen, Proceedings, Series B 73: 169-195.
Koiter, W. (1970b) On the mathematical foundation of shell theory. In: Proc. Int. Congr. Math., Nice 3: 123-130.
Krätzig, W. (1980) On the structure of consistent linear shell theories. In: Koiter, W., Mikhailov, G. (Eds.). Theory of Plates and Shells: 353-368. North-Holland, Amsterdam.
Lekhnitskii, S.G. (1981) Theory of elasticity of an anisotropic elastic body. Moscow: Mir Publishers.
Levinson, M. (1985) The simply supported rectangular plate: An exact, three dimensional, linear elasticity solution. J. Elasticity, 15: 283-291.
Liu, Z., Wang, C., Duan, G., Tan, J. (2019) A new refined plate theory with isogeometric approach for the static and buckling analysis of functionally graded plates. Int. J. Mech. Sci. 161-162: 105036.
Naghdi, P. M. (1963) Foundations of elastic shell theory. In: Sneddon, I, Hill, R. (Eds.) Progress in Solid Mechanics 4, North-Holland, Amsterdam: 1-90.
Nematzadeh, M., Eskandari-Ghadi, M., Navayi Neya, B. (2012) An analytical solution for transversely isotropic simply supported thick rectangular plates using displacement potential functions. Journal of Strain Analysis 46: 121-142.
Nicotra, V., Podio Guidugli, P., Tierro, A. (1999) Exact equilibrium solutions for linear elastic plate-like bodies. Journal of Elasticity 56: 231-245.
Nowacki, W. (1954) The stress function in three-dimensional problems concerning an elastic body characterized by transverse isotropy. Bulletin de l'Academie Polonaise Sciences 2: 21-25.
Pruchnicki, E. (2014) Two-dimensional model of order h5 for the combined bending, stretching, transverse shearing and transverse normal stress effects of homogeneous plates derived from three-dimensional elasticity. Math. Mech. Solids 19: 477-490.
Reissner, E. (1944) On the theory of bending of elastic plates. J. Math. Phys. 23: 184-191.
Reissner, E. (1945) On the effect of transverse shear deformation on the bending of elastic plates. J. Appl. Mech. 12: 69-77.

Saidi, A. R., Atashipour, S. R., Jomehzadeh, E. (2009) Reformulation of Navier equations for solving three-dimensional elasticity problems with applications to thick plate analysis. Acta Mech. 208: 227-235.
Schneider, P., Kienzler, R., Böhm, M. (2014) Modelling of consistent second-order plate theories for anisotropic materials. Z. Angew. Math. Mech. 94: 21-42.
Schneider, P., Kienzler, R. (2017) A Reissner-type plate theory for monoclinic material derived by extending the uniform-approximation technique by orthogonal tensor decompositions of *n*th-order gradients. Mechanica 52: 2143-2167.
Steigmann, D. J. (2008) Two-dimensional models for the combined bending and stretching of plates and shells based on three-dimensional linear elasticity. Int. J. Engng. Sci. 46: 654-676.
Steigmann, D. J. (2012) Refined theory of linear elastic plates: Laminae and laminates. Math. Mech. Solids 17: 351-363.
Szabo, I. (1987) Geschichte der mechanischen Prinzipien. Birkhäuser, Basel.
Tran, H.Q., Vu, V.T., Tran, M.T., Nguyen-Tri, P. (2019) A new four-variable refined plate theory for static analysis of smart laminated functionally graded carbon nanotube reinforced composite plates. Mechanics of Materials 142: 103294.
Vekua, I. (1955) On one method to calculating prismatic shells (In Russian). Trudy Tbilisi. Mat. Inst. 21: 191-259.
Vekua, I. (1985) Shell theory: general methods of construction. Monographs, Advanced Texts and Surveys in Pure and Applied Mathematics. John Wiley & Sons, New York.
Wang, J., Steigmann, D., Wang, F.F., Dai, H.H. (2018) On a consistent finite-strain plate theory of growth. J. Mechanics Physics Solids 111: 184-214.
Wang, F.F., Steigmann, D.J., Dai, H.H. (2019) On a uniformly-valid asymptotic plate theory. Int. J. of Non-Linear Mech. 112: 117-125.
Youngdahl, C.K. (1969) On the completeness of a set of stress functions appropriate to the solutions of elasticity problems in general cylindrical co-ordinates. Int. J. Eng. Sci. 7: 61-79.

Appendix

In Section 4, we developed the solution of the three-dimensional theory of elasticity for the boundary-value problem (2.5) based on Elliot's displacement potentials ϕ_i (Elliot, 1948). Reference to this solution will be given in the following by (KK).

We are aware of two further solutions for the same problem. Nicotra et al. (1999), in the following abbreviated by (NPT), extended the classical Levinson solution (Levinson, 1985) for transversely isotropic materials and considered the same simply supported plate continuum under sinusoidal loads.

On the other hand, in Nematzadeh et al. (2012), in the following abbreviated by (NEN), a solution is provided based on two potential representations F and χ of the Lekhnitskii-Hu-Nowacki solution (Lekhnitskii, 1981; Hu, 1953; Nowacki, 1954). For the boundary-value problem under consideration, it turns out that χ is identically zero and F has to satisfy a quasi-biharmonic differential equation.

All three quite different approaches are claimed as exact three-dimensional solutions of the three-dimensional linear theory of elasticity of one and the same boundary-value problem. Thus, due to the uniqueness requirements established by Kirchhoff (1859), they must be identical. It is the object of this Appendix to show this identity since it is not at all obvious from the provided formulae in the different approaches.

The three approaches rely on the solution of a characteristic equation. In KK we have (4.3)

$$C_{11}C_{44}\theta^2 + \left[C_{13}(2C_{44}+C_{13}) - C_{11}C_{33}\right]\theta + C_{33}C_{44} = 0. \tag{A.1}$$

With (3.2), the two solutions

$$\theta_{1,2} = \frac{1}{2}\left[\frac{C_{11}^*C_{33} - 2C_{44}C_{13}}{C_{11}C_{44}} \pm \sqrt{\left(\frac{C_{11}^*C_{33} - 2C_{44}C_{13}}{C_{11}C_{44}}\right)^2 - 4\frac{C_{33}}{C_{11}}}\right] \tag{A.2}$$

are transformed to new constants λ_1 and λ_2 by

$$\lambda_\alpha = \frac{\kappa}{\sqrt{\theta_\alpha}}, \qquad \alpha = 1,2$$

with (A.3)

$$\kappa = \sqrt{\left(\frac{m\pi}{a}\right)^2 + \left(\frac{n\pi}{b}\right)^2} = \frac{1}{a}\sqrt{(m\pi)^2 + (n\pi\alpha)^2} = \frac{1}{a}\gamma_{mn}$$

(cf. 2.2e). From simple algebra, it follows

$$\lambda_1^2 \cdot \lambda_2^2 = \kappa^4 \frac{C_{11}}{C_{33}}, \tag{A.4}$$

$$\lambda_1^2 + \lambda_2^2 = \kappa^2 \frac{C_{11}^* C_{33} - 2C_{44}C_{13}}{C_{33}C_{44}},$$

and we find from (A.2)

$$\lambda_{1,2}^2 = \frac{1}{2}\kappa^2 \left[\frac{C_{11}^* C_{33} - 2C_{44}C_{13}}{C_{33}C_{44}} \mp \sqrt{\left(\frac{C_{11}^* C_{33} - 2C_{44}C_{13}}{C_{33}C_{44}} \right)^2 - 4\frac{C_{11}}{C_{33}}} \right]. \tag{A.5}$$

With (A.4), the following identities can be proved easily

$$\begin{aligned}
&\frac{\lambda_1^2 C_{33} - \kappa^2 C_{44}}{\kappa^2(\lambda_1^2 C_{33} + \kappa^2 C_{13})} = \frac{C_{44} + C_{13}}{\lambda_2^2 C_{33} + \kappa^2 C_{13}}, \\
&\frac{\lambda_2^2 C_{33} - \kappa^2 C_{44}}{\kappa^2(\lambda_2^2 C_{33} + \kappa^2 C_{13})} = \frac{C_{44} + C_{13}}{\lambda_1^2 C_{33} + \kappa^2 C_{13}}, \\
&\frac{\lambda_1^2}{\kappa^2(\lambda_1^2 C_{13} + \kappa^2 C_{11})} = \frac{1}{\lambda_2^2 C_{33} + \kappa^2 C_{13}}, \\
&\frac{\lambda_2^2}{\kappa^2(\lambda_2^2 C_{13} + \kappa^2 C_{11})} = \frac{1}{\lambda_1^2 C_{33} + \kappa^2 C_{13}}, \\
&\lambda_1^2 C_{11}C_{13} + \kappa^2 C_{11}^2 - \frac{\lambda_2^2 \lambda_1^2}{\kappa^2} C_{13}C_{44} - \lambda_2^2 C_{11}C_{44} \\
&= \frac{\lambda_1^2 \lambda_2^2}{\kappa^4}(C_{13} + C_{44})(\lambda_1^2 C_{33} + \kappa^2 C_{13}), \\
&\lambda_2^2 C_{11}C_{13} + \kappa^2 C_{11}^2 - \frac{\lambda_1^2 \lambda_2^2}{\kappa^2} C_{13}C_{44} - \lambda_1^2 C_{11}C_{44} \\
&= \frac{\lambda_1^2 \lambda_2^2}{\kappa^4}(C_{13} + C_{44})(\lambda_2^2 C_{33} + \kappa^2 C_{13}).
\end{aligned} \tag{A.6}$$

which will be used in the following.

The constants in the displacement solution (KK) (4.10) with (4.8) can now readily be evaluated in terms of λ_α and C_{AB}

$$\begin{aligned}
&k_1 = \frac{C_{33}\lambda_2^2 - \kappa^2 C_{44}}{\kappa^2(C_{44} + C_{13})}, \qquad k_2 = \frac{C_{33}\lambda_1^2 - \kappa^2 C_{44}}{\kappa^2(C_{44} + C_{13})}, \\
&\beta_1 = \frac{C_{33}\lambda_2^2 + C_{13}\kappa^2}{\kappa^2(C_{44} + C_{13})} \lambda_1 \cosh\left(\frac{1}{2}\lambda_1 h \right), \\
&\beta_2 = \frac{C_{33}\lambda_1^2 + C_{13}\kappa^2}{\kappa^2(C_{44} + C_{13})} \lambda_2 \cosh\left(\frac{1}{2}\lambda_2 h \right), \\
&\beta_3 = \kappa^2 A(\lambda_1, \lambda_2, h) \frac{C_{11}^* C_{33}}{C_{13} + C_{44}},
\end{aligned} \tag{A.7}$$

with

$$A(\lambda_1,\lambda_2,h)=\lambda_2\cosh\left(\frac{1}{2}\lambda_2 h\right)\sinh\left(\frac{1}{2}\lambda_1 h\right)-\lambda_1\sinh\left(\frac{1}{2}\lambda_2 h\right)\cosh\left(\frac{1}{2}\lambda_1 h\right), \tag{A.8}$$

and the displacements are calculated as

$$u_\alpha=\frac{1}{2}q_{mn}\frac{C_{13}+C_{44}}{C_{44}A(\lambda_1,\lambda_2,h)}\begin{Bmatrix}\dfrac{m\pi}{a}\cos(m\pi\xi_1)\sin(n\pi\alpha\xi_2)\\ \dfrac{n\pi\alpha}{a}\sin(m\pi\xi_1)\cos(n\pi\alpha\xi_2)\end{Bmatrix}$$
$$\left\{\lambda_2\frac{\cosh(\frac{1}{2}\lambda_1 h)\sinh(\lambda_1 a\zeta)}{\lambda_2^2C_{33}+\kappa^2C_{13}}-\lambda_1\frac{\cosh(\frac{1}{2}\lambda_1 h)\sinh(\lambda_2 a\zeta)}{\lambda_1^2C_{33}+\kappa^2C_{13}}\right\}, \tag{A.9}$$

$$u_3=\frac{1}{2}q_{mn}\frac{\lambda_1\lambda_2(C_{13}+C_{44})}{A(\lambda_1,\lambda_2,h)C_{44}}\sin m\pi\xi_1\sin n\pi\alpha\xi_2$$
$$\left\{\frac{\cosh\left(\frac{1}{2}\lambda_2 h\right)\cosh(\lambda_1 a\zeta)}{\lambda_1^2C_{33}+\kappa^2C_{13}}-\frac{\cosh\left(\frac{1}{2}\lambda_1 h\right)\cosh(\lambda_2 a\zeta)}{\lambda_2^2C_{33}+\kappa^2C_{13}}\right\} \tag{A.10}$$

with λ_α given by (A.5). Equation (A.9) and (A.10) coincide with (5.3) and (5.4), respectively.

NEN use the same Voigt notation as (3.1). We merely have to replace in (1 NEN)

$$A_{AB}=C_{AB}\qquad A,B=1,2,...,6. \tag{A.11}$$

The characteristic equation (8 NEN) reads

$$C_{33}C_{44}s^4+\left(C_{13}(2C_{44}+C_{13})-C_{11}C_{33}\right)s^2+C_{11}C_{44}=0. \tag{A.12}$$

For reason of comparison, we divide (A.12) by s^4 yielding

$$C_{11}C_{44}\frac{1}{s^4}+\left(C_{13}(2C_{44}+C_{13})-C_{11}C_{33}\right)\frac{1}{s^2}+C_{33}C_{44}=0. \tag{A.13}$$

Thus we identify

$$\begin{aligned}s_1&=\frac{1}{\sqrt{\theta_2}}=\frac{1}{\kappa}\lambda_2,\\ s_2&=\frac{1}{\sqrt{\theta_1}}=\frac{1}{\kappa}\lambda_1.\end{aligned} \tag{A.14}$$

After adjusting the notation

$$\begin{aligned} &B_1 = \frac{m\pi}{a}, \quad B_2 = \alpha\frac{n\pi}{a}, \quad B_3 = \kappa \\ &\lambda = \kappa h, \qquad x = a\xi_1, \qquad y = a\xi_2, \quad z = a\zeta, \end{aligned} \tag{A.15}$$

the displacements (NEN 32a) read

$$\begin{aligned} u_\alpha = -2\frac{q_{mn}}{\gamma_1}\frac{C_{13}+C_{44}}{\kappa^2} &\left\{ \begin{matrix} \frac{m\pi}{a}\cos(m\pi\xi_1)\sin(n\pi\alpha\xi_2) \\ \alpha\frac{n\pi}{a}\sin(m\pi\xi_1)\cos(n\pi\alpha\xi_2) \end{matrix} \right\} \\ &\left\{ \lambda_2(\lambda_1^2 C_{13} + \kappa^2 C_{11})\cosh\left(\frac{1}{2}\lambda_1 h\right)\sinh(a\lambda_2\zeta) \right. \\ &\left. -\lambda_1(\lambda_2^2 C_{13} + \kappa^2 C_{11})\cosh\left(\frac{1}{2}\lambda_2 h\right)\sinh(a\lambda_1\zeta) \right\}, \end{aligned} \tag{A.16}$$

$$\begin{aligned} u_3 = 2\frac{q_{mn}}{\gamma_1}&\sin m\pi\xi_1 \sin n\pi\alpha\xi_2 \\ &\left\{ -\left(\lambda_1^2 C_{11}C_{13} + \kappa^2 C_{11}^2 - \frac{1}{\kappa^2}\lambda_2^2\lambda_1^2 C_{13}C_{44} - \lambda_2^2 C_{11}C_{44} \right)\cosh\left(\frac{1}{2}\lambda_1 h\right)\cosh(a\lambda_2\zeta) \right. \\ &\left. +\left(\lambda_2^2 C_{11}C_{13} + \kappa^2 C_{11}^2 - \frac{1}{\kappa^2}\lambda_1^2\lambda_2^2 C_{13}C_{44} - \lambda_1^2 C_{11}C_{44} \right)\cosh\left(\frac{1}{2}\lambda_2 h\right)\cosh(a\lambda_1\zeta) \right\}, \end{aligned} \tag{A.17}$$

where

$$\begin{aligned} \gamma_1 = -4C_{44}\kappa^3 &\frac{1}{\kappa^4}(\lambda_1^2 C_{13} + \kappa^2 C_{11})(\lambda_2^2 C_{13} + \kappa^2 C_{11})\frac{\kappa}{\lambda_1\lambda_2} \\ &\left\{ \lambda_1 \sinh\left(\frac{1}{2}\lambda_2 h\right)\cosh\left(\frac{1}{2}\lambda_1 h\right) - \lambda_2\cosh\left(\frac{1}{2}\lambda_2 h\right)\sinh\left(\frac{1}{2}\lambda_1 h\right) \right\} \end{aligned}$$

which can be rearranged with (A.8) as

$$\gamma_1 = +\frac{4}{\lambda_1\lambda_2}C_{44}A(\lambda_1,\lambda_2,h)(\lambda_1^2 C_{13} + \kappa^2 C_{11})(\lambda_2^2 C_{13} + \kappa^2 C_{11})$$

and further with (A.6 c. d) to

$$\gamma_1 = +\frac{4}{\lambda_1\lambda_2}C_{44}A(\lambda_1,\lambda_2,h)\frac{\lambda_1^2\lambda_2^2}{\kappa^4}(\lambda_1^2 C_{33} + \kappa^2 C_{13})(\lambda_2^2 C_{33} + \kappa^2 C_{13}). \tag{A.18}$$

Introducing (A.6 c. d) and (A.6 e. f) into (A.16) and (A.17), respectively, and using (A.18), the relations for u_α and u_3 of the equations (A.9) and (A.10) are recovered, respectively.

Next we turn our attention to NPT. The stress-strain relation is given in symbolic notation (5.1 NPT)

$$\begin{aligned}
&\mathbb{S} = 2\bar{\mu}\mathbb{PEP} + \bar{\lambda}(\mathbb{P}\cdot\mathbb{E})\mathbb{P} + \tau_1(\mathbb{P}^{\perp}\cdot\mathbb{E})\mathbb{P}^{\perp} \\
&+\tau_2\left((\mathbb{P}^{\perp}\cdot\mathbb{E})\mathbb{P} + (\mathbb{P}\cdot\mathbb{E})\mathbb{P}^{\perp}\right) \\
&+2\tau_3\left((\mathbb{C}_1\cdot\mathbb{E})\mathbb{C}_1 + (\mathbb{C}_2\cdot\mathbb{E})\mathbb{C}_2\right),
\end{aligned}$$

where

$$\begin{aligned}
&\mathbb{P} = \vec{c}_1 \otimes \vec{c}_1 + \vec{c}_2 \otimes \vec{c}_2 \\
&\mathbb{P}^{\perp} = \vec{z} \otimes \vec{z} \\
&\mathbb{C}_{\alpha} = \sqrt{2}\ \text{sym}\left[\vec{c}_{\alpha} \otimes \vec{z}\right] \qquad \alpha = 1,2.
\end{aligned}$$

The unit vectors $(\vec{c}_1, \vec{c}_2, \vec{z})$ form an orthogonal Cartesian frame with coordinates $(x_1 = a\xi_1, x_2 = a\xi_2, x_3 = a\zeta)$.. We transform the symbolic notation into our index notation and identify

$$\begin{aligned}
&C_{11} = C_{22} = 2\bar{\mu} + \bar{\lambda}, \\
&C_{33} = \tau_{1,} \\
&C_{44} = C_{55} = \tau_3, \\
&C_{66} = \frac{1}{2}(C_{11} - C_{22}) = \bar{\mu}, \\
&C_{13} = C_{23} = \tau_2, \\
&C_{AB} = 0 \quad \text{otherwise.}
\end{aligned} \tag{A.19}$$

The characteristic equation (5.11,12 NPT) is given as

$$\beta^4 - s\kappa^2\beta^2 + p\kappa^4 = 0$$

with

$$\begin{aligned}
&s = \frac{\tau_1(\bar{\lambda} + 2\bar{\mu}) - \tau_2(\tau_2 + 2\tau_3)}{\tau_1\tau_3}, \\
&p = \frac{\bar{\lambda} + 2\bar{\mu}}{\tau_1},
\end{aligned} \tag{A.20}$$

and κ as introduced in (A.3b).

Avoiding confusion with β_i (A.7), we define

$$\beta = \eta,$$

introduce (A.19), multiply by $C_{33}C_{44}/\eta^4$ and find

$$C_{11}C_{44}\frac{\kappa^4}{\eta^4}+\left[C_{13}(2C_{44}+C_{13})-C_{11}C_{33}\right]\frac{\kappa^2}{\eta^2}+C_{33}C_{44}=0. \tag{A.21}$$

Comparison with (A.1) leads to the identification

$$\eta=\frac{\kappa}{\sqrt{\theta}}, \tag{A.22}$$

and finally to

$$\begin{aligned}\lambda_1^2&=\eta_2^2,\\ \lambda_2^2&=\eta_1^2.\end{aligned} \tag{A.23}$$

The solution of our boundary value problem is given by (2.9 NPT)

$$\begin{aligned}u_\alpha&=-g(\zeta)w(\xi_1,\xi_2)_{,\alpha},\\ u_3&=f(\zeta)w(\xi_1,\xi_2)\end{aligned} \tag{A.24}$$

with (5.14 NPT)

$$\begin{aligned}f(a\zeta)&=\tilde{K}_1\cosh(a\lambda_2\zeta)+\tilde{K}_2\sinh(a\lambda_2\zeta)+\tilde{K}_3\cosh(a\lambda_1\zeta)+\tilde{K}_4\sinh(a\lambda_1\zeta)\\ g(a\zeta)&=\tilde{L}_1\cosh(a\lambda_2\zeta)+\tilde{L}_2\sinh(a\lambda_2\zeta)+\tilde{L}_3\cosh(a\lambda_1\zeta)+\tilde{L}_4\sinh(a\lambda_1\zeta).\end{aligned} \tag{A.25}$$

From the boundary conditions at the upper and lower faces of the plate, the constants are evaluated. $\tilde{K}_2,\tilde{K}_4,\tilde{L}_1$ and $\tilde{L}_3$ vanish and the remaining constants are expressed with (A.19) as

$$\begin{aligned}\tilde{K}_1&=-\frac{1}{2}q_{mn}\frac{\lambda_1\lambda_2(C_{44}+C_{13})}{C_{44}(\lambda_2^2C_{33}+\kappa^2C_{13})}\;\frac{\cosh\left(\frac{1}{2}\lambda_1h\right)}{A(\lambda_1,\lambda_2,h)},\\ \tilde{K}_3&=+\frac{1}{2}q_{mn}\frac{\lambda_1\lambda_2(C_{44}+C_{13})}{C_{44}(\lambda_1^2C_{33}+\kappa^2C_{13})}\;\frac{\cosh\left(\frac{1}{2}\lambda_2h\right)}{A(\lambda_1,\lambda_2,h)},\\ \tilde{L}_2&=-\tilde{K}_1\frac{\lambda_2^2C_{33}-\kappa^2C_{44}}{\kappa^2\lambda_2(C_{13}+C_{44})},\\ \tilde{L}_4&=-\tilde{K}_3\frac{\lambda_1^2C_{33}-\kappa^2C_{44}}{\kappa^2\lambda_1(C_{13}+C_{44})},\end{aligned} \tag{A.26}$$

and $A(\lambda_1,\lambda_2,h)$ as given by (A.8)

Introducing (A.26) and (A.25) into (A.24) and using the identities (A.6 a, b) we arrive exactly at (A.9) and (A.10). Thus it has been shown that all three approaches lead to one and the same result.

In NPT, results for an isotropic material response are also given. It can be shown that the displacements coincide with the solution of Saidi et al. (2009) and the solution based on Youngdahl's displacement potentials (Youngdahl, 1969) presented in Kienzler and Kashtalyan (2020).